Thesis for The Degree of Doctor of Philosophy

Propeller-Hull Interaction Effects in Calm Water and Regular Head Waves

Mohsen Irannezhad

Department of Mechanics and Maritime Sciences
Chalmers University of Technology
Gothenburg, Sweden, 2024

Propeller-Hull Interaction Effects in Calm Water and Regular Head Waves

Mohsen Irannezhad

ISBN 978-91-8103-004-4
Doktorsavhandlingar vid Chalmers tekniska högskola, Ny serie nr 5462.
ISSN 0346-718X

Department of Mechanics and Maritime Sciences
Division of Marine Technology
Chalmers University of Technology
SE-412 96 Göteborg,
Sweden
Phone: +46(0)31 772 1000

Printed by Chalmers Digitaltryck,
Gothenburg, Sweden 2024.

Propeller-Hull Interaction Effects in Calm Water and Regular Head Waves

Mohsen Irannezhad

Department of Mechanics and Maritime Sciences
Chalmers University of Technology

Abstract

In order to design fuel-efficient ships and install compatible propulsion systems, ship and propeller designers need to know the potential effects of the interactions between different ship components, e.g., hull, propeller, appendages and machinery, on the ship performance at sea. Neglecting the interaction effects may result in unbalanced powering which adversely affects the energy/fuel consumption, hence increasing ships operational cost and environmental impact. Developing accurate and reliable engineering methods that can predict the ships required power considering the interaction effects, can be an important contribution to achieve the aforementioned needs of the shipping industry.

Traditionally, power prediction has been carried out for ships operating in calm water rather than more realistic environmental conditions. However, waves can play a crucial role on the ship performance at sea. The interactions between waves, hull and the propulsion system of a ship may significantly affect the ship motions, resistance, wake, speed and propeller/engine load in comparison to calm water operational conditions. Nonetheless, it is practically impossible to take all of the entailed interactions between different ship components into consideration within the process of power prediction in all possible operational and environmental conditions, hence a series of assumptions and simplifications are often introduced.

In this thesis, as a step towards the ship power prediction in more realistic environmental conditions, the propeller-hull interaction effects in a range of selective operational conditions in calm water and regular head waves are considered in model-scale. The main objective is to perform numerical investigations of the ship performance in these conditions, aiming at understanding the involved flow physics in the propeller-hull interaction effects on the ship behavior and its propulsion characteristics. The investigations in both calm water and regular head waves are carried out in three distinctive steps: only the bare hull consideration, only the propeller consideration known as propeller open water (POW) and finally, for the self-propelled hull. The bare hull investigations incorporate employing two computational methods: a Fully Nonlinear Potential Flow (FNPF) panel method and a state-of-the-art Computational Fluid Dynamics (CFD) method using a Reynolds-Averaged Navier-Stokes (RANS) approach. However, for the POW and self-propulsion studies only the RANS approach is employed. A formal verification and validation (V&V) procedure is applied to understand and control the numerical and modeling errors in the RANS computations.

Overall, the results of the employed numerical methods were in good

agreement with the experimental data. The analysis of the results provided valuable insight into the ship and propeller hydrodynamic performance in terms of the ship motions, resistance, wake, propeller characteristics and the correlations between them. The ship hydrodynamics analyses from this thesis can shed more light onto the propeller-hull interaction effects in waves and help the ship/propeller designers optimize their designs for more realistic conditions than only calm water.

Keywords

CFD, RANS, FNPF, EFD, Regular Head Waves, Ship Motions, Resistance, Nominal Wake, Propeller Open Water Characteristics, Taylor Wake Fraction, Thrust Deduction Factor, Self-Propulsion Point of Model

List of Publications

Appended publications

This thesis consists of an extended summary and the appended papers listed below.

Paper I Irannezhad, M., Eslamdoost, A., Kjellberg, M., and Bensow, R. E. (2022a). "Investigation of ship responses in regular head waves through a Fully Nonlinear Potential Flow approach". *Ocean Engineering* 246. https://doi.org/10.1016/j.oceaneng.2021.110410

Paper II Irannezhad, M., Bensow, R. E., Kjellberg, M., and Eslamdoost, A. (2021). "Towards uncertainty analysis of CFD simulation of ship responses in regular head waves". In: *Proceedings of the 23rd Numerical Towing Tank Symposium (NuTTS 2021)*. Duisburg, Germany, pp. 37–42. https://www.uni-due.de/imperia/md/content/ist/nutts_23_2021_mulheim.pdf

Paper III Irannezhad, M., Bensow, R. E., Kjellberg, M., and Eslamdoost, A. (2023). "Comprehensive computational analysis of the impact of regular head waves on ship bare hull performance". *Ocean Engineering* 288. https://doi.org/10.1016/j.oceaneng.2023.116049

Paper IV Irannezhad, M., Kjellberg, M., Bensow, R. E., and Eslamdoost, A. (2024a). "Experimental and numerical investigations of propeller open water characteristics in calm water and regular head waves". *Preprint Under Review in Ocean Engineering, available at SSRN*. http://doi.org/10.2139/ssrn.4706213. https://ssrn.com/abstract=4706213

Paper V Irannezhad, M., Kjellberg, M., Bensow, R. E., and Eslamdoost, A. (2024b). "Impacts of Regular Head Waves on Thrust Deduction at Model Self-Propulsion Point". *Manuscript*

Other publications

In addition to the appended papers, I have authored or co-authored the following publications/reports. However, they are not appended to this thesis, due to contents overlapping that of appended papers or contents not directly related to the thesis.

Publication A Irannezhad, M., Eslamdoost, A., and Bensow, R. E. (2019a). "Numerical investigation of a general cargo vessel wake in waves". In: *Proceedings of the 22nd Numerical Towing Tank Symposium (NuTTS 2019)*. Tomar, Portugal. http://web.tecnico.ulisboa.pt/ist12278/NuTTS2019/Session1/Session1_2.pdf

Publication B Irannezhad, M., Eslamdoost, A., and Bensow, R. E. (2019b). "Numerical investigation of a large diameter propeller emergence risk for a vessel in waves". In: *Proceedings of the 8th International Conference on Computational Methods in Marine Engineering (MARINE 2019)*. Gothenburg, Sweden, pp. 634–645. https://doi.org/10.5281/zenodo.2650219

Publication C Irannezhad, M. (2022). "Numerical investigation of ship responses in calm water and regular head waves". Thesis for the degree of Licentiate of Engineering, Report no. 2022:04, Department of Mechanics and Maritime Sciences, Chalmers University of Technology. ISSN: 1652-8565. https://research.chalmers.se/publication/530499/file/530499_Fulltext.pdf

Publication D Irannezhad, M., Kjellberg, M., Bensow, R. E., and Eslamdoost, A. (2022b). "Propeller open water characteristics in waves". In: *Proceedings of the 24th Numerical Towing Tank Symposium (NuTTS 2022)*. Zagreb, Croatia, pp. 36–41. https://drive.google.com/file/d/1Fw1qI6Fb9nQPP7p0QSAUMJ8yYRBBjYAy/view

Publication E Eslamdoost, A., Irannezhad, M., and Bensow, R. E. (2023). "The Dynamics of a Ship Nominal Wake in Head Waves". In: *The 10th International Conference on Computational Methods in Marine Engineering (MARINE 2023)*. http://doi.org/10.23967/marine.2023.129

Acknowledgment

This thesis is based on research carried out at the Division of Marine Technology, Department of Mechanics and Maritime Sciences at Chalmers University of Technology and funded by The Swedish Transport Administration through Lighthouse (Swedish Maritime Competence Center). The simulations were performed on the resources provided by the National Academic Infrastructure for Supercomputing in Sweden (NAISS) and the Swedish National Infrastructure for Computing (SNIC) at Chalmers Centre for Computational Science and Engineering (C3SE) and National Supercomputer Center at Linköping University (NSC). I would like to express my sincere appreciation to Professor Yasuyuki Toda from Osaka University for generously sharing a significant amount of experimental data for the KVLCC2 tanker. The Maritime Research Institute Netherlands (MARIN) is also acknowledged for providing the experimental data for the LDP vessel.

My heartfelt gratitude goes to those who made my PhD research possible. Special thanks to my main supervisor, Arash Eslamdoost, for his unwavering encouragement, support and guidance. His technical expertise and timely assistance were invaluable, especially during challenging moments. I am also thankful to my co-supervisor and examiner, Rickard Bensow, for his valuable guidance and concise feedback that significantly contributed to my research. I appreciate the assistance and insightful discussions from co-supervisor Martin Kjellberg at RISE - SSPA. Lastly, I would like to express my gratitude for the support from my manager, Jonas Ringsberg, throughout these years.

I want to express gratitude to my current and former colleagues at Chalmers for fostering a positive work environment. Thank you, Debarshee, Saeed, Mohammad (the junior), Daniel, Qais, Rui, Chengqian, Marily, Stephan, Kourosh, Carlo and Franz for the enjoyable moments and fun lunch hours. Special thanks also go to my caring friends Mohammad (the senior), Ioli and Mehmet for sharing the best-ever vibes in the office atmosphere.

Finally, I would like to thank my supportive parents who have always devoted themselves to me, my role model brothers Mike and Masoud for always being on my side, my beloved wife Rojin for her patience, kindness and endless support in my ups and downs, Minoo, Siamak, Arash and my friends Mohammad, Alireza, Homayoon, Ashkan, Negin, Maryam, Asal, Farzad, Rojan, Masoud, Sahar, Jesus, Karen, Mohsen, Rasool, Setareh, Ehsan, Amal, Afshin, Sasy, Majid and Mahish for positive energy.

Mohsen Irannezhad
Göteborg, February 2024

Nomenclature

$1 + k$	Form factor (-)
$\bar{\psi}$	Mean value of the quantity under study in Fourier analysis
$\ddot{x}$	Surge acceleration (m/s^2)
ΔC_F	Roughness allowance (-)
η_D	Propulsive efficiency (-)
η_H	Hull efficiency (-)
η_O	Open water efficiency (-)
η_R	Relative rotative efficiency (-)
λ	Wave length (m)
μ	Heading angle (deg)
ν	Kinematic viscosity of water (m^2/s)
ω_E	Encounter wave frequency (rad/s)
ω_w	Wave frequency (rad/s)
$\psi(t)$	Time series of the quantity under study in Fourier analysis
ψ_i	The ith harmonic amplitude of quantity under study in Fourier analysis
$\psi_{\varepsilon i}$	The ith harmonic phase of quantity under study in Fourier analysis
ρ	Water density (kg/m^3)
θ	Pitch motion (deg)
$\tilde{u}$	Surface-averaged axial velocity component of nominal wake over propeller disk (m/s)
$\tilde{v}$	Surface-averaged transversal velocity component of nominal wake over propeller disk (m/s)
$\tilde{w}$	Surface-averaged vertical velocity component of nominal wake over propeller disk (m/s)
A	Wave amplitude $H/2$ (m)
B	Ship breadth at mid-ship (m)
C_A	Incremental resistance coefficient for model-ship correlation (-)
C_T	Total resistance coefficient (-)
C_{AW}	Added wave resistance coefficient (-)
C_F	Frictional resistance coefficient (-)
D	Propeller diameter (m)
F_0	External constant towing force (N)
F_D	Skin friction correction force (N)
Fr	Froude number (-)

g	Gravitational acceleration (m/s^2)
H	Wave height (m)
J	Advance ratio (-)
K	Spring stiffness (N/m)
K_Q	Torque coefficient (-)
k_s	Roughness of the hull surface (m)
K_T	Thrust coefficient (-)
L	Ship length (m)
L_{wl}	Waterline length (m)
m_3	Light-weight carriage mass (kg)
n	Grid refinement level (-)
n^{POW}	Propeller rotational speed in open water condition (rps)
n^{SP}	Propeller rotational speed in self-propulsion condition (rps)
P_D	Delivered Power (W)
P_E	Effective power (W)
Q	Propeller torque (Nm)
R	Propeller radius (m)
r	Radial position (m)
R_F	Frictional resistance (N)
R_P	Pressure resistance (N)
R_S	Shear resistance (N)
R_T	Total resistance (N)
R_V	Viscous resistance (N)
R_W	Wave making resistance (N)
R_{AW}	Added resistance due to waves (N)
Re	Reynolds number (-)
S_{wet}	Wetted surface area at rest (m^2)
T	Propeller thrust (N)
t	Thrust deduction factor (-)
T_E	Wave encounter period (s)
T_{spring}	Spring natural period (s)
U	Ship velocity (m/s)
u	Axial velocity components of nominal wake (m/s)
u_a	Effective wake (advance) velocity (m/s)
v	Transversal velocity components of nominal wake (m/s)
w	Vertical velocity components of nominal wake (m/s)
w_T	Taylor wake fraction (-)
x	Surge motion (m)
z	Heave motion (m)

Contents

Part I

Summary

Chapter 1

Introduction

Although shipping is the most efficient and cost-effective mode of cargo transportation, maritime transport is still considered a rather large source of greenhouse gas emissions worldwide. Increasing environmental societal awareness and concerns, and strict international regulations regarding emissions from shipping to the sea and air, stimulate further technological developments and energy efficiency improvements in the shipping industry.

Reducing the operational power of ships is one of the main measures that is also motivated by ship owners to reduce their fleet fuel consumption and costs. The maritime community has been in the process of developing various concepts for optimizing ships to operate at their most efficient and economical operational point. However, the application of such optimizations needs accurate and reliable predictions of ships' required power in the design process. Inaccurate predictions can lead to unbalanced powering that would adversely affect the energy/fuel consumption, hence increasing ships operational cost and environmental impact. Therefore, prediction of the required operational power would be beneficial for the overall assessment of a ship performance.

Traditionally, power prediction has been conducted for ships operating in calm water. However, calm water is rather an exception during an actual voyage. Ships may experience involuntary/voluntary speed loss when they operate in a more realistic environmental condition than calm water. Various factors responsible for the loss of speed in a seaway are mentioned by Bhattacharyya (1978) as added resistance due to waves, wind and ship motions, loss of propulsive efficiency (related to propeller underload/overload, altered conditions affecting the characteristics of the propulsive machinery and variation of wake into the propeller due to motions, speed loss as well as propeller ventilation/emergence) and voluntary reduction of engine speed for preventing green water, slamming, excessive accelerations, propeller racing or course keeping.

Therefore, ship designers consider an additional experience-based reserved power of $15-25\%$, called "sea margin" ITTC (2017a), to ensure reliable performance of ships in other environmental conditions than calm water. While this practice has demonstrated its adequacy in predicting power requirements for numerous vessels over the years, it can potentially result in underpower/overpower

situations as the ships may seldom encounter such severe conditions. Currently, there is a growing trend toward ship design optimization in operational conditions closer to near-service conditions than calm water, which is also the main motivation in this thesis.

Waves play a significant role in affecting most of the aforementioned factors responsible for ship speed loss. Operating in waves may have several effects on ship hydrodynamic behavior. The interactions between waves, hull and the propulsion system of a ship may significantly affect the ship motions, resistance, wake and propeller/engine load in comparison to calm water operational conditions. Added resistance due to waves and the variation of propulsive factors for a ship operating in real sea conditions affect its required engine power in comparison to the idealistic calm water conditions, which may lead to a noticeable ship performance degradation. Moreover, large amplitude ship motions in a rough sea may adversely affect the ship structural integrity and harm the crew and cargo. Therefore, ship performance prediction in waves is crucial, especially in the early stages of the ship design process.

Ship hydrodynamic performance prediction in calm water and waves has been widely investigated through experimental, empirical and numerical methods in literature. However, it is practically impossible to take all of the entailed physics into consideration in these methods, hence, a series of assumptions and simplifications are often introduced. Bertram (2012) has presented a structured overview of the most well-known ship performance prediction methods.

Ship hydrodynamic performance can be predicted experimentally through Captive, Semi-captive or Free-Sailing (Free-Running) tests in towing tanks or seakeeping basins, ITTC (2017b). Although these model tests are expensive and time-consuming, the ship hydrodynamic performance is expected to be predicted with a high level of accuracy from the measurements.

On the other hand, empirical methods often rely on statistical correlations derived from experimental data, providing a cheaper and faster way of estimating ship behavior, whereas they may lack the precision and accuracy of more complex methods.

Since the 1950s, computational seakeeping methods have started to evolve. Each method has a different level of fidelity with respect to its computational costs and accuracy. Generally, the approach in these methods is based on either Potential Flow methods (Strip Theory, Vortex Methods or Three-Dimensional Panel Methods) or Computational Fluid Dynamics (CFD) techniques.

Usually, potential flow solvers are computationally much faster than CFD solvers. In potential flow methods, the flow is assumed to be inviscid, incompressible and irrotational. Generally, empirical values for some viscous effects can play a complementary role in these methods. In the cases where the viscous effects are insignificant, the application of potential flow methods may provide a great advantage in terms of computational efficiency.

Contrary to potential flow methods, the state-of-the-art CFD methods have the advantage of predicting ship hydrodynamic responses more accurately by conducting high fidelity nonlinear computations with fewer simplifications related to the flow physics. However, these methods are computationally expensive and time-consuming. The most common CFD methods in the

context of ship hydrodynamics are based on the so-called Reynolds-Averaged Navier-Stokes (RANS) approach.

Depending on the specific problem under study, the level of required details and the available resources, one should choose a suitable method for the ship performance prediction. Generally, one major advantage of numerical methods over model tests is the possibility of acquiring in-depth information about the fluid flow, which is challenging, costly and extremely cumbersome to achieve through model tests, if even possible. Common practices often involve a combined approach, utilizing both model tests and numerical predictions. The numerical results are then validated using the experimental measurements and subsequently analyzed to extract and gain detailed information about the ship hydrodynamic performance. Today, with the development of advanced computational tools and the availability of extensive computing power, the application of numerical methods for the investigations of ship performance prediction in waves is gradually gaining more popularity.

1.1 Scope

A seaway may contain waves with various heights and lengths propagating in different directions, hence for a full analysis of ship performance in waves, a broad range of environmental and operational conditions have to be considered. Moreover, the ship hydrodynamic responses may be subject to various correlated factors originating from the interaction effects between different ship components (e.g., hull, propeller, appendages and engine) in such environmental and operational conditions. These turn the full analysis of ship performance in waves into an extremely cumbersome, if not impossible, task. However, from a hydrodynamic engineering perspective, the focus lies on understanding the flow physics around a ship in waves. Therefore, as with any engineering approach, it is essential to simplify the problem in the initial step and comprehend the underlying physical phenomena in simplified scenarios before extending the analysis to more complex circumstances.

A proper candidate for the initial stages of investigations, which is opted for in this thesis, is to study the propeller-hull interaction effects on the ship performance in calm water and regular head waves. Disregarding the interaction effects imposed by machinery and all other appendages except the propeller reduces the complexity of the interaction effects between the hull and propeller as the primary ship components. Furthermore, only the regular head waves are taken into account due to their comparatively simpler impacts on the hull and propeller hydrodynamic performance and the involved flow physics, e.g., initiating primarily surge, heave and pitch, as the key entailed motions and relatively less sophisticated wake field encountered by the propeller. The investigations of the propeller-hull interaction effects in calm water and regular head waves can provide valuable insight into the impacts of waves on the ship hydrodynamic performance, hence contributing to the more efficient ship powering in the near-service scenarios. The main research question to examine in this thesis is the impacts of regular head waves on the propeller-hull

interaction effects in comparison to calm water operational conditions.

1.2 Objectives

The key objectives of this thesis are:

- to map the factors contributing to the hydrodynamics of propeller-hull interaction effects in regular head waves and gain insight into the associated flow physics;
- to compare the propeller-hull interaction effects on the ship performance in calm water and regular head waves;
- to comprehend the challenges of propeller performance in regular head waves and identify potential design constraints imposed by the flow dynamics;
- to assess the application of computational methods with different levels of fidelity and their correspondence with experimental methods.

These are achieved through performing numerical investigation of ship and propeller in calm water and regular head waves. Then the results are validated against experimental measurements and an extensive analysis of the associated flow physics using the computational results is carried out. This study may provide a clearer understanding of ship hydrodynamic performance in a more realistic condition which may be beneficial for ship/propeller designers to optimize their designs or introduce new technological solutions. Consequently, such advancements can contribute to various aspects of the marine industry including environmental impacts, as well as, economic considerations and safety-related measures.

1.3 Delimitation

The scope and objectives of the current thesis concern ship performance in calm water and regular head waves, disregarding the interactions imposed by machinery and other appendages except propeller. Given that the focus lies on understanding the flow hydrodynamics, solely a limited number of case studies, i.e., ship and propeller geometries, operational conditions (ship velocity, loading condition and propeller rotational speed), environmental and wave conditions (wave length and wave height), are considered.

Moreover, the investigations in this thesis concern only ship hydrodynamic performance in model-scale, where the experimental tests are carried out under a more controlled environment in comparison to full scale sea trials. This choice ensures a more credible flow analysis. Furthermore, the studies are conducted for ships free in three degrees of freedom (3DOF), i.e., surge, heave and pitch.

A fully nonlinear potential flow method (SHIPFLOW MOTIONS) and a RANS-based CFD method (STAR-CCM+) together with towing tank tests are employed for understanding the flow hydrodynamics.

1.4 Methodology

In order to obtain a clearer understanding of the impact of waves on the propeller-hull interactions, first, the influence of regular head waves on each component (propeller or hull) is studied separately. This allows for isolating the effects of waves on the propeller and hull performance before diving into analysing the more intricate combined interaction effects. Therefore, the investigations are carried out in three distinctive steps as follows:

1. analysis of the bare hull in calm water and regular head waves;
2. analysis of the propeller open water performance in calm water and regular head waves;
3. analysis of the self-propelled hull in calm water and regular head waves.

A schematic representation of these steps is shown in Figure 1.1. The bare hull investigations in step 1, illustrated in Figures 1.1(a) and 1.1(b), are conducted using two different computational methods: a Fully Nonlinear Potential Flow (FNPF) panel method and a CFD method using a RANS approach.

The utilization of the FNPF method is found to be beneficial for investigations of the bare hull motions and resistance in calm water and regular head waves, as the main ship motions are surge, heave and pitch which are found to be less affected by viscosity. This enables investigations in a broader range of operational conditions due to the lower computational demand in the FNPF solver. The results of such studies are used to understand the overall behavior of the hull in regular head waves with regards to the ship motions and resistance as well as their correlation.

Thereafter, a RANS solver is employed in order to study the bare hull performance, because the investigations in Step 1 focus not only on the ship motions and resistance but also its nominal wake. The RANS solver is capable of predicting the complex interactions between the boundary layer and incident waves and providing comprehensive flow field information, which is not achievable in the FNPF method. Prior to the hull performance investigations in regular head waves, a numerical wave propagation study is carried out in an empty computational domain in the absence of the hull to examine the quality of regular head waves in the RANS computations relative to the corresponding analytical waves.

Through comparison of the bare hull behavior in regular head waves to that of calm water, the effects of such waves on the bare hull hydrodynamic performance are examined. A general overview of the physical aspects of different contributing factors is obtained.

While the operational condition for a ship's propeller is inherently complex due to the ship motions and wake variations, it remains necessary to study the propeller performance under controlled operational conditions to gain insights into performance deviations in the challenging conditions encountered behind the hull. A set of model tests as well as RANS computations are

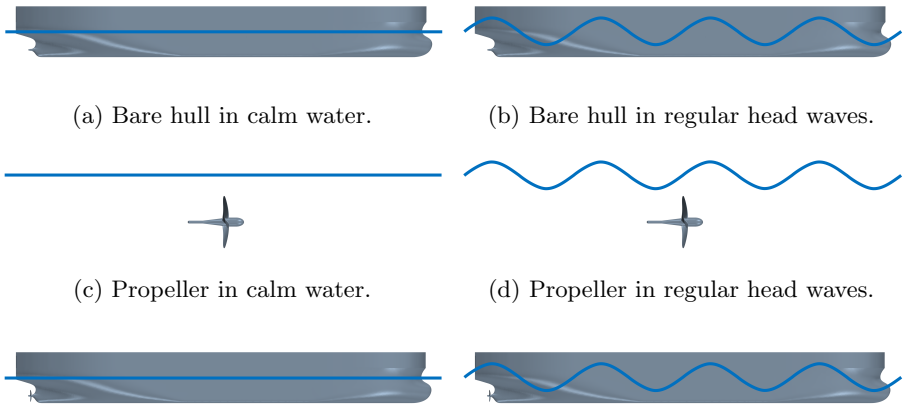

(a) Bare hull in calm water.

(b) Bare hull in regular head waves.

(c) Propeller in calm water.

(d) Propeller in regular head waves.

(e) Self-propulsion in calm water.

(f) Self-propulsion in regular head waves.

Figure 1.1: Schematic decomposition of the research conducted in the thesis.

conducted in order to perform the Propeller Open Water (POW) investigations in calm water and regular head waves in step 2, depicted in Figures 1.1(c) and 1.1(d). The evaluated impacts of regular head waves on the POW performance provide primary insights into the propeller performance characteristics such as thrust, torque and efficiency and the deviations with respect to the calm water condition.

In the final step of the investigations, step 3 shown in Figures 1.1(e) and 1.1(f), the performance of the self-propelled ship in calm water and regular head waves is examined using the RANS solver. The knowledge gained in the previous steps helps the analysis of the impact of regular head waves on the propeller-hull interactions.

Before analyzing the hydrodynamic performance of the hull and propeller using the achieved numerical results in these three steps, comprehensive validation of the employed numerical tools is carried out using a collection of experimental data corresponding to the respective conditions. It is worth mentioning that the experimental measurements of the POW investigations in step 2 are carried out within the framework of the current thesis, while the remaining experimental data is acquired from other sources.

A formal verification and validation (V&V) procedure is applied in order to understand and control the numerical and modeling uncertainties/errors in the RANS computations. Verification is a purely mathematical exercise that intends to show that we are solving the equations right, whereas validation is an engineering practice that intends to show that we are solving the right equations, Roache (1998). In this thesis, the main focus of the verification (uncertainty analysis) is on systematic grid convergence study.

The novelty of this thesis can be characterized through its concise and comprehensive approach to explaining the flow physics involved in the impacts

of waves on ship hydrodynamic performance. The investigations begin at the component level, addressing the isolated effects of waves on the hull and propeller, and conclude with a holistic perspective examining their interaction effects.

1.5 Thesis Outline

This thesis consists of two parts: an extended summary followed by five appended papers. The appended papers present the detailed investigations associated with the employed approach and its intermediate steps. The extended summary part briefly presents the content of each paper and then explains the interconnections between them as well as the thesis objectives. A general overview of the investigations covering both calm water and regular head wave conditions presented in the appended papers reads as follows,

Paper I bare hull hydrodynamics using the FNPF solver;

Paper II wave propagation investigation in the RANS solver;

Paper III bare hull hydrodynamics using the RANS solver;

Paper IV POW studies through model tests and the RANS solver;

Paper V self-propulsion hydrodynamics using the RANS solver.

The extended summary, following the present chapter, is organized as follows.

In Chapter 2, a brief background of the ship performance evaluation is described, focusing mainly on the propeller-hull interaction effects in calm water and regular head waves. Moreover, the post-processing techniques utilized in the papers are shortly explained. The holistic overview of the correlations between the results derived from different papers is also elaborated.

In Chapter 3, the objectives and summary of the findings for each appended paper are presented.

Last but not least, Chapter 4 is devoted to the concluding remarks proceeded from the studies performed in the thesis.

Chapter 2

Ship Performance Evaluation

In this thesis, the ship performance evaluation is carried out with respect to the ship hydrodynamic performance in calm water and regular head waves. In this chapter, the important contributing factors to the ship hydrodynamic performance and the relevant prediction methods are briefly explained with the main focus on the propeller-hull interaction effects on the ship performance.

The ship performance evaluation concerns the propulsion characteristics which depend on the bare hull performance, propeller open water performance and self-propulsion performance. In the following, the superscripts "BH", "POW" and "SP" represent the bare hull, propeller open water and self-propulsion conditions, respectively.

The propulsive efficiency η_D is often considered the ultimate element in the ship performance evaluation and is defined as the ratio of the effective power P_E (power required to move bare hull at a given speed) and the delivered power P_D (shaft power into propeller) as,

$$\eta_D = \frac{P_E}{P_D} = \frac{R_T^{BH} U}{2\pi Q^{SP} n^{SP}}, \tag{2.1}$$

in which R_T^{BH} is the bare hull total resistance at the ship velocity U, but Q^{SP} and n^{SP} are the propeller torque and rotational speed in the self-propulsion condition to drive the ship at this velocity. The prediction of propulsive efficiency η_D is very complicated as it is affected by various factors related to the hull and propeller hydrodynamics and their interactions. Moreover, the scale effects (model-scale or full-scale) as well as the environmental conditions in which the ship is operating (calm water or waves) add to the complexity of such predictions.

There are different techniques and assumptions in the performance predictions using experimental or numerical methods. Given that the chosen approach in this thesis includes bare hull, propeller open water and self-propulsion performance in calm water and regular head waves, the applied prediction methods

and the entailed flow physics considerations are explained in the following.

2.1 Regular Waves Propagation

For a ship operating in waves, the main excitation forces exerted on the hull are induced by the encountered waves. Therefore, the attribute and quality of encountered waves significantly affect the ship performance in waves. Obtaining high-quality regular waves is a well-known challenge in both experimental tests as well as numerical simulations, ITTC (2021a,b).

The wave generation in towing tanks or seakeeping basins is often calibrated, prior to the ship performance model tests, to ensure high-quality propagating waves. However, the quality of the propagating waves in each test might vary depending on various factors, for instance, the wave maker performance or the pause time between two consecutive tests. This may then result in lower levels of reliability with respect to the discrepancies between the actual wave in experiments and the intended one.

Generally, the propagating regular head waves in the FNPF method are rather equivalent to their analytical counterpart. However, the quality of the propagating waves in the RANS solver depends significantly on the modeling parameters. As it is mentioned by Perić and Abdel-Maksoud (2018, 2020), Berndt et al. (2021) and Perić et al. (2022) case-dependent parameters should be tuned for minimizing the reflections from the boundaries of the computational domain and improving the numerical simulations of flows with free surface waves.

In order to investigate the modeling errors involved in the simulation of wave propagation and achieve a robust simulation setup for wave propagation in the employed RANS solver, a comprehensive study is performed in Paper II. Later, the investigations underwent a refinement in Publication C, Irannezhad (2022), but the conclusions remained unchanged, hence Paper II is appended to this thesis to present the wave propagation studies. The aim was to minimize the modeling errors of wave propagation (e.g., amplitude reduction and period change during propagation, disturbances (wiggles) on the free surface and reflection at boundaries) and compare the discrepancies from the analytical wave. Different modeling parameters are hence tuned in the RANS solver to derive high-quality regular waves related to the current investigations.

In the studies carried out in the appended papers, the dependency of different ship performance quantities on the encountered wave height H is examined by deriving the non-dimensional quantities taking into account the actual measured wave height from each respective model test measurement. Nevertheless, the analytical wave height was used for the non-dimensionalization of the numerical results, due to the expected insignificant deviations between numerical and analytical waves. The validation errors for both dimensional and non-dimensional quantities are calculated and compared in different conditions. In a similar approach by Sigmund (2019), lower validation errors are observed for the non-dimensional resistance and motions in comparison to the dimensional ones.

2.2 Bare Hull Performance

The bare hull hydrodynamic performance can be mainly characterized through its motions, resistance and nominal wake. The key motions are the surge x, heave z and pitch θ. Resistance is the horizontal force opposing the steady forward motion of the hull. These are often derived at different ship forward speeds U, which can also be presented based on the Froude number Fr as,

$$Fr = \frac{U}{\sqrt{gL}} \tag{2.2}$$

in which L is the ship length and g is the gravitational acceleration.

Nominal wake is the velocity distribution of the flow at the propeller disk, even though there is no actual propeller installed for the bare hull investigations. The propeller disk is a circular surface with the same radius as the propeller and with its origin at the propeller center while moving with the hull and hence following the ship motions. The velocity distribution on the propeller disk is affected by the presence of the hull and its motions as well as the incident flow field. The nominal wake is very important for the design of wake-adapted propellers as the velocity distributions significantly affect the propeller performance. The nominal wake measurements in model tests, for instance by using the Stereo Particle Image Velocimetry (SPIV), vane wheels or pitot tubes, are often expensive and time-consuming. However, the nominal wake can often be extracted effortlessly from the CFD simulations.

The motions, resistance and nominal wake for a hull operating in waves deviate from those of calm water. The investigations in Paper I and Paper III concern the bare hull performance in calm water and regular head waves.

2.2.1 Bare Hull in Calm Water

The experimental methods for prediction of the bare hull performance in calm water are presented in the recommended procedures and guidelines ITTC (2021c) from the International Towing Tank Conference (ITTC). The model-scale hull is towed with the desired ship velocity U in the towing tanks and its total resistance R_T^{BH} and motions are measured.

From both experimental and numerical computations, the time series of resistance and motions in calm water are derived and subsequently post-processed by time-averaging the values over a defined time window to extract a single value for each quantity.

Based on the decomposition of resistance in the ITTC-78 method given in ITTC (2021d), the total resistance is divided into a viscous resistance component $R_V = (1 + k)R_F$, which includes the form effect on friction and pressure, and a wave making resistance component R_W as,

$$R_T^{BH} = (1 + k)R_F + R_W. \tag{2.3}$$

The form factor $1 + k$ can be determined from low speed tests or numerical computations, and its derivation includes various challenges mentioned by

Korkmaz (2023), which are out of the scope of the current thesis. The frictional resistance R_F can be computed from,

$$R_F = \frac{1}{2}\rho S_{wet} U^2 C_F, \tag{2.4}$$

in which ρ is the water density and S_{wet} is the wetted surface area at rest. The frictional resistance coefficient C_F can be estimated from the ITTC-57 model-ship correlation line,

$$C_F = \frac{0.075}{(\log Re - 2)^2}, \tag{2.5}$$

where $Re = UL/\nu$ is the Reynolds number, in which ν is the kinematic viscosity of water. The extrapolation to full-scale total resistance can be done using the 1978 ITTC Performance Prediction Method, ITTC (2021d). However, since the investigations in this thesis only concern the model-scale condition, the extrapolation methods are not further explained here.

In the numerical investigations conducted in Paper I, a Fully Nonlinear Potential Flow (FNPF) panel method is employed in which the flow is assumed to be homogeneous, inviscid, incompressible and irrotational. The wave breaking or fragmentation of the fluid domain (e.g., green water on deck) cannot be modeled in this method. The unsteady hydrodynamic pressure is calculated at any point in the domain from the unsteady Bernoulli equation and the hydrodynamic forces and moments acting on the body are computed by integration of the hydrodynamic pressure over the hull surface. The detailed description of the method is provided in Paper I and also by Kjellberg (2013). Since FNPF is an inviscid method, only the wave making resistance component R_W can be computed from this method.

In the numerical investigations conducted in Paper III, a CFD method (RANS) is employed. The calm water total resistance computed from this method can be directly compared to that of model tests. The total resistance can also be divided into a pressure resistance component R_P which is the normal forces on the hull and a shear resistance component $R_S = R_F$ which is the tangential forces on the hull as mentioned by Larsson and Raven (2010). These components can be directly extracted from the RANS computations.

2.2.2 Bare Hull in Regular Head Waves

ITTC (2021e) provides the experimental methods for the prediction of the bare hull performance in regular head waves. Similar to calm water, the model is towed in waves at the desired velocity and the resistance and motions are measured. As mentioned before, the key induced motions by the regular head waves are the surge, heave and pitch, hence other motions are often restrained. Moreover, the majority of experiments are carried out with the surge motion restrained as well (2DOF), since the effects of surge motion on resistance in waves are assessed to be relatively low, for instance by Sadat-Hosseini et al. (2013). However, surge motion can play a crucial role in the coupling between motions as well as the variation of wake at the propeller

disk as mentioned by Ueno et al. (2013). Therefore, the surge motion effects on the wake characteristics should not be overlooked. One of the techniques to include the surge motion of the bare hull operating in regular head waves at the expected velocity is through using a weak spring system connected to the carriage in the test setup. This setup is explained in Paper III and the investigations in this paper consider the hull free to surge (3DOF) employing the weak spring system.

From the model tests and computations in regular head waves, the time series of various quantities are derived. In order to post-process the time series of different quantities $\psi(t)$, the common practice is to perform Fourier analysis as,

$$\psi(t) = \bar{\psi} + \psi_1 \cos(\omega_E t + \psi_{\varepsilon 1}) + \psi_2 \cos(2\omega_E t + \psi_{\varepsilon 2}) + \psi_3 \cos(3\omega_E t + \psi_{\varepsilon 3}) + ..., \quad (2.6)$$

where $\bar{\psi}$ is the mean value and ψ_i is the ith harmonic amplitude of the quantity under study ψ, $\psi_{\varepsilon i}$ is the phase component related to the ith harmonic amplitude and ω_E is the wave encounter frequency calculated for each wave based on its respective wave frequency ω_w, the heading angle $\mu = 180°$ as,

$$\omega_E = \omega_w - \frac{{\omega_w}^2 U}{g} \cos(\mu). \quad (2.7)$$

The wave encounter period $T_E = 2\pi/\omega_E$ can be derived from wave encounter frequency. In the investigations carried out in this thesis, various cautions are taken into account for defining the time window for the Fourier analysis in order to diminish the post-processing uncertainties. The details are included in the appended papers, but a brief explanation is provided here.

The main consideration is to use a time window that is equal to an integer number multiplied by T_E (multiple of T_E) to minimize the spectral leakage in the Fourier analysis. The choice of integer number varies in different investigations and wave conditions. The main challenge is when there is a weak spring system involved, hence the ship behavior consists of extra harmonic components in the spring natural frequency aside from the wave encounter frequency. Although a good choice of the time window should include several spring natural periods, this is not feasible due to the extremely high required computational costs. Therefore, for each wave length λ, the time window is selected in a way to have an integer number of T_E which is closest to one spring natural period T_{spring} as an attempt towards incorporating the spring effects.

In order to analyze the instantaneous values of different quantities and their correlations during the wave encounter, the reconstructed time series are generated. The reconstructed time series are derived for 1 encountered wave period T_E in each wave. The reconstruction is based on the Fourier series, Equation 2.6, in which only the dominant harmonic components (HC), i.e., harmonic amplitudes (HA) and harmonic phases, derived from the Fast Fourier Transform (FFT) results over the chosen time window, are taken into account. The same time origin $t/T_E = 0$ is considered for the reconstructed time series of different quantities.

In Paper I, a broad range of operational conditions are considered taking advantage of the relatively lower computational costs involved in the FNPF method. The dominant harmonic amplitudes of motions and wave making resistance are compared at different conditions and the correlations between them are identified. The FNPF results are also compared to the experimental data (EFD). However, the EFD data in regular head waves from Paper I are derived in the self-propulsion conditions and different assumptions are considered to estimate the wave making resistance from the thrust measurements. These assumptions are explained in Section 2.4.2.

In Paper III, due to the higher computational costs of RANS simulations, the investigations are carried out in a limited number of operational conditions. The formal Verification and Validation (V&V) procedure is carried out. The main focus of such verification (uncertainty analysis) is on systematic grid convergence study. The dominant harmonic amplitudes as well as the reconstructed time series of motions, resistance and nominal wake are analyzed in detail. The dimensional and non-dimensional quantities are compared between CFD and EFD. The computed nominal wake is also validated using SPIV measurements from the experiments.

It is worth mentioning that the investigations in Paper II, aside from the wave propagation studies, include the initial attempts to study the bare hull performance in regular head waves. At the time of publication of this paper, the choices of the FFT time window and the post-processing techniques were still under discussion. Subsequent decisions were made later and the hull performance investigations in this paper were further developed in Paper III. Therefore, the most complete version of the bare hull performance RANS results in regular head waves can be found in Paper III, whereas the wave propagation investigations are covered in Paper II.

One of the key aspects of the bare hull performance in regular head waves is the added resistance due to waves R_{AW} which is derived from subtracting the calm water resistance from the mean resistance in waves. For the potential flow investigations in Paper I, the added wave making resistance is considered as the total added wave resistance, and the change of form factor and the frictional component of added resistance are assumed negligible. However, the total added resistance is derived in Paper III considering both the pressure and shear components.

The added wave resistance coefficient C_{AW} is derived from,

$$C_{AW} = \frac{R_{AW}}{\rho g B^2 A^2 / L}, \tag{2.8}$$

in which B is the hull breadth at mid-ship and $A = H/2$ is the encountered wave amplitude.

2.3 Propeller Open Water Performance

The Propeller Open Water (POW) performance can be characterized mainly through its thrust T^{POW}, torque Q^{POW} and open water efficiency η_O^{POW}.

There are limitations in the literature for propeller performance deviations in waves in comparison to calm water conditions and the majority of investigations focus on the POW in calm water. Even when the POW in waves is studied, the majority of the investigations focus on the free surface effects related to propeller ventilation or emergence. Therefore, the impacts of regular head waves on the POW performance under fully submerged and non-ventilating conditions are mainly overlooked.

In Paper IV, such impacts are studied through both experimental and numerical (RANS) methods. Different advance ratios $J^{POW} = U^{POW}/n^{POW}D$ are considered, in which D is the propeller diameter, n^{POW} is the propeller rotational speed and U^{POW} is the advance velocity (carriage speed in model tests) in the POW condition. The advance ratios, wave conditions (wave length and wave height) and submergence depths are selected in order to avoid propeller ventilation and to ensure that the propeller is fully-submerged during the whole wave encounter period, while still experiencing the effect of the incident waves.

For the POW performance investigations in Paper IV, a constant advance velocity U^{POW} is considered, which represents the ship velocity of the respective hull U in the bare hull investigations in Paper III and self-propulsion investigations in Paper V. The aim was to perform the POW performance evaluation of the propeller under a similar operational condition as the propeller experiences behind the self-propelled hull, but disregarding the hull interaction effects. Detailed analyses of the flow physics are carried out using the RANS simulations. Moreover, laminar to turbulent transition of the flow, as one of the influential associated factors in the POW performance, is investigated briefly in Paper IV.

2.3.1 POW in Calm Water

ITTC (2021f) provides the experimental methods for POW in calm water. In towing tank experiments, the propeller is mounted on a drive shaft while being equipped with a hub cap and moving with the carriage.

The desired advance ratios are commonly obtained in two ways: either by keeping the carriage speed constant and adjusting the propeller rotational speed or by keeping the propeller rotational speed constant and adjusting the carriage speed. The important difference between these two conditions is the difference in Reynolds number and hence flow regime on the blades.

Although the Reynolds number in full-scale propellers often leads to a fully turbulent flow regime, the Reynolds number in model-scale propellers may approach the laminar flow range. There are recommendations from ITTC regarding the minimum Reynolds number consideration for the POW model tests intended for full scale predictions. The main point is that the laminar flow dominance for the constant carriage speed cases is more probable as the Reynolds number in these cases is rather low. However, as mentioned before, the aim in Paper IV is to investigate the propeller performance under a similar operational condition as the propeller experiences behind the self-propelled hull, but disregarding the hull interaction effects. Therefore, the advance speed

(carriage speed) is defined to represent the respective ship speed in Paper III and Paper V. Consequently, the dominance of the laminar flow regime becomes crucially important in the POW performance investigations. In Paper IV such flow regime effects are briefly investigated.

From the POW studies, the open water thrust and torque coefficients, i.e., K_T^{POW} and K_Q^{POW}, are defined as,

$$K_T^{POW} = \frac{T^{POW}}{\rho n^{POW\,2} D^4}, \qquad K_Q^{POW} = \frac{Q^{POW}}{\rho n^{POW\,2} D^5}. \tag{2.9}$$

The propeller open water efficiency η_O^{POW} is then calculated as,

$$\eta_O^{POW} = \frac{J^{POW}}{2\pi} \frac{K_T^{POW}}{K_Q^{POW}}. \tag{2.10}$$

The thrust coefficient, torque coefficient and propeller open water efficiency are then plotted for different advance ratios, hence forming the propeller open water curves.

The computational results of the RANS simulations for the thrust, torque and efficiency are compared to those of EFD data in Paper IV in a selected number of advance ratios. The numerical investigations consist of the fully turbulent simulations as well as the simulations incorporating transition models.

2.3.2 POW in Regular Head Waves

The experimental and numerical investigations of the POW in regular head waves are carried out similarly to those of calm water and the details are provided in Paper IV. Various wave conditions are considered and the effects of different waves on the POW performance are analyzed. The Fourier analysis is carried out and the dominant harmonic amplitudes as well as the reconstructed time series of thrust, torque and efficiency are studied. In addition to the integral forces and moments, the single-blade load variations are also studied where the oscillations in the propeller frequency are discussed.

2.4 Self-Propulsion Performance

The self-propulsion performance of a propeller-appended hull is often characterized through the propeller thrust T^{SP} and torque Q^{SP} as well as the ship motions. The propeller thrust and torque from the self-propulsion condition can be combined with the bare hull and propeller open water properties in order to define the propulsion characteristics of the ship. The propeller-hull interactions, as the main focus of this thesis, are primarily conceived through the thrust deduction and wake fraction.

The required thrust T^{SP} to drive a self-propelled ship at a velocity U is higher than the bare hull resistance R_T^{BH} at that velocity. This originates from the propeller-induced acceleration (suction) of the flow and hence the change of the pressure distribution at the aft-ship (close to the propeller) in self-propulsion. It is more reasonable to consider the effects of the propeller

behind the hull as causing an increase in resistance. However, it is also common practice to formulate this resistance increase as a deduction from the thrust available at the propeller, i.e., to assume that only part of the propeller thrust is available to overcome the bare hull resistance. The increase of resistance or deduction of thrust in self-propulsion is often presented through thrust deduction factor t as,

$$t = \frac{T^{SP} - R_T^{BH}}{T^{SP}} = 1 - \frac{R_T^{BH}}{T^{SP}}. \tag{2.11}$$

The wake field (velocity distribution) encountered by the propeller behind the hull significantly affects the propeller performance, which in return affects the hull performance and consequently affects the wake field again. In order to describe the wake velocity (advance velocity) u_a relevant for the propeller in relation to the ship velocity U, the effective wake fraction (Taylor wake fraction w_T in Taylor notation, ITTC (2021g)) is defined as,

$$w_T = 1 - \frac{u_a}{U}. \tag{2.12}$$

Therefore, the velocity distribution at the aft-ship crucially affects both the thrust deduction and wake fraction, leading to complex propeller-hull interaction effects on the ship performance.

In order to obtain a deeper understanding of the propulsion characteristics and power prediction, the propulsive efficiency η_D in Equation 2.1, can be extended by Q^{POW}/Q^{POW} and re-arranged after replacing $R_T^{BH} = T^{SP}(1-t)$ and $U = u_a/(1-w_T)$ as,

$$\eta_D = \frac{R_T^{BH} U}{2\pi Q^{SP} n^{SP}} \frac{Q^{POW}}{Q^{POW}} = \frac{T^{SP} u_a}{2\pi Q^{POW} n^{SP}} \frac{Q^{POW}}{Q^{SP}} \frac{(1-t)}{(1-w_T)}. \tag{2.13}$$

Accordingly, the propeller open water efficiency η_O, relative rotative efficiency η_R and hull efficiency η_H can be defined as,

$$\eta_O = \frac{T^{SP} u_a}{2\pi Q^{POW} n^{SP}}, \tag{2.14}$$

$$\eta_R = \frac{Q^{POW}}{Q^{SP}}, \tag{2.15}$$

$$\eta_H = \frac{(1-t)}{(1-w_T)}. \tag{2.16}$$

There also exist the shafting and gearing efficiencies that contribute to the propulsive efficiency, but these machinery-related factors are disregarded in this thesis.

Based on the ITTC recommended procedures and guidelines, ITTC (2014, 2021d,h), the effective wake velocity u_a is usually obtained using the thrust identity method (or torque identity method). In the thrust identity method, the thrust at the self-propulsion condition is assumed to be equal to the thrust

from the open water condition. According to this assumption, the propeller generates the same thrust at the same rotational speed when: working behind a hull at the speed of U and in open water at the speed of u_a. Consequently, the thrust coefficient from the self-propulsion condition K_T^{SP},

$$K_T^{SP} = \frac{T^{SP}}{\rho {n^{SP}}^2 D^4}, \tag{2.17}$$

is used to read off J^{POW}, K_Q^{POW} and η_O^{POW} from the propeller open water curves. Then the effective wake velocity u_a is derived from,

$$u_a = J^{POW} n^{SP} D, \tag{2.18}$$

and the effective wake fraction w_T is then calculated as,

$$w_T = 1 - \frac{J^{POW} n^{SP} D}{U}. \tag{2.19}$$

Therefore, $\eta_O = \eta_O^{POW}$ is the open water efficiency based on the thrust obtained in the self-propulsion conditions. The relative rotative efficiency $\eta_R = Q^{POW}/Q^{SP} = K_Q^{POW}/K_Q^{SP}$ represents the relation between the propeller torque in self-propulsion and open water conditions. The hull efficiency η_H describes the influence of the propeller-hull interaction on the efficiency of the propulsion system. The magnitude of the propulsive efficiency η_D often gets affected more significantly by the propeller open water efficiency than the relative rotative efficiency and hull efficiency as mentioned by Saettone (2020).

ITTC (2021d) outlines the procedures for scaling the self-propulsion characteristics from model-scale to full-scale. The focus of this thesis is solely on the model-scale condition, hence the scaling methods are not further elaborated here. Nevertheless, it is crucial to address a notable aspect of the self-propulsion conditions in model-scale. The self-propulsion investigations require finding the operational point at which the ship resistance and propeller thrust are in equilibrium. The skin friction coefficient C_F is different between model-scale and full-scale, leading to a significant difference in the propeller loading between these conditions and hence affecting the propeller and ship performance.

The common practice in model-scale self-propulsion investigations usually accounts for the theoretically correct propeller loading in model-scale to justify reliable scaling results. This correction is usually applied through an external tow force in model-scale self-propulsion conditions, called skin friction correction force F_D, to unload the propeller. When this force is considered, the operational point is called "the self-propulsion point of the ship" (ship SPP), and it should be considered for the derivation of the thrust deduction factor t, hence modifying Equation 2.11 to,

$$t = 1 - \frac{R_T^{BH} - F_D}{T^{SP}}. \tag{2.20}$$

The skin friction correction force F_D is estimated in various ways in the literature, for instance, through the newest ITTC definition provided in ITTC (2021h) and ITTC (2021d) as,

$$F_D = \frac{1}{2}\rho_m U_m^2 S_{wet_m}(C_{F_m} - (C_{F_s} + \Delta C_F + C_A)), \tag{2.21}$$

and compared to the older ITTC definitions of F_D in the final report of the latest conference ITTC (2021i). The subscript "m" and "s" represent the model-scale and full-scale values, respectively. The roughness allowance ΔC_F and the incremental resistance coefficient for model-ship correlation C_A (correlation allowance) are defined as,

$$\Delta C_F = 0.044((\frac{k_s}{L_{wl}})^{1/3} - 10Re^{-1/3}) + 0.000125, \tag{2.22}$$

$$C_A = (5.68 - 0.6\log Re) \times 10^{-3}, \tag{2.23}$$

in which k_s indicates the roughness of the hull surface and L_{wl} is the waterline length. Additionally, in ITTC (2021h) the estimation of F_D including the form factor is provided as,

$$F_D = \frac{1}{2}\rho_m U_m^2 S_{wet_m}((1+k)(C_{F_m} - C_{F_s}) - \Delta C_F - C_A)). \tag{2.24}$$

Furthermore, Lee et al. (2019) and Seo et al. (2020) used slightly different equation,

$$F_D = \frac{1}{2}\rho_m U_m^2 S_{wet_m}((1+k)(C_{F_m} - C_{F_s}) - \Delta C_F)). \tag{2.25}$$

Cai et al. (2023) calculated F_D from,

$$F_D = \frac{1}{2}\rho_m U_m^2 S_{wet_m}(C_{F_m} - C_{F_s}). \tag{2.26}$$

Sigmund (2019) calculated F_D from,

$$F_D = \frac{1}{2}\rho_m U_m^2 S_{wet_m}(C_{T_m} - C_{T_s}), \tag{2.27}$$

in which instead of frictional resistance coefficient, the total resistance coefficient C_T is used,

$$C_T = \frac{R_T}{0.5\rho S_{wet} U^2}. \tag{2.28}$$

Moreover, Bhattacharyya and Steen (2014) utilized the following equation for the estimation of F_D,

$$F_D = \frac{1}{2}\rho_m U_m^2 S_{wet_m}(1+k)(C_{F_m} - (C_{F_s} + \Delta C_F)), \tag{2.29}$$

where ΔC_F is estimated from,

$$\Delta C_F = (110.31(k_s U_s)^{0.21} - 403.33) \times C_{F_s}^2, \tag{2.30}$$

which is different from the ITTC equation for roughness allowance. The estimated F_D from these equations in the literature results in remarkably different values, hence leading to distinct shifting of the propeller loading and uncertainty in the self-propulsion point of the ship (ship SPP).

The selection of the target self-propulsion point regime for a ship operating in waves depends on the adopted method for the power prediction in waves as described in ITTC (2021j). In the ship SPP, it is often assumed that F_D is similar between calm water and waves, as the averaged frictional resistance per encountered wave period is assumed to remain identical to the calm water frictional resistance. However, based on the investigations carried out in Paper III, it is seen that this assumption is not valid as the frictional component of the added resistance due to waves is determined to be considerable. This introduces an additional uncertainty to the correct propeller loading consideration in waves in the case of ship SPP.

In the self-propulsion investigations in Paper V, the propeller-hull interaction effects are examined at the self-propulsion point of the model (model SPP) considering $F_D = 0$ N in order to eliminate the aforementioned uncertainties related to the propeller loading involved in the application of F_D. This choice is yet in line with the objectives of the thesis, as the main aim is to study the flow physics and how it affects the propeller-hull interactions in regular head waves in comparison to calm water. Therefore, since the investigations only concern the model-scale conditions, the consideration of the model SPP for the analysis of the flow physics appears coherent. In this way, the common assumption in the added power prediction methods on equal thrust deduction factor and wake fraction in calm water and waves, e.g., in the Thrust and Revolution Method (TNM) as well as the Resistance and Thrust Identity Method (RTIM) in ITTC (2021j), can be examined. However, it should be kept in mind that at the self-propulsion point of the model (model SPP), the propeller is highly loaded which may result in amplification of the propeller-hull interaction effects when compared to the full-scale.

The investigations in Paper III and Paper V concern the ship free to surge by means of a weak spring system. In the corresponding model tests, the model was free to surge while it was towed with a light-weight carriage connected to the main carriage through the weak spring system. The occurrence of surge resonance, i.e., interference of the spring natural frequency with the surge motion frequency in the studied waves, was prevented by the choice of a suitable spring stiffness K. In order to avoid large stretch/compression of the spring, an external constant force F_0 (estimated from a set of preliminary model tests) was considered in each model test, but the details of which are missing in the experimental reports.

In the RANS simulations in Paper III and Paper V, in addition to the constant force F_0, the effects of the spring system, i.e., light-weight carriage (with the mass of m_3) and spring (with the stiffness of K) which were part of the experimental setup, are replicated through application of external light-weight carriage force $-m_3\ddot{x}$ and spring force $-Kx$ in the ship advancing direction at the center of gravity (COG) of the ship. $\ddot{x}$ is the instantaneous surge acceleration and x is the instantaneous surge motion, hence positive surge x

results in spring compression and thus a negative spring force $-Kx$ (i.e., in the opposite direction of ship forward speed).

An ideal propeller-hull interactions analysis may include the derivation of instantaneous thrust deduction and wake fraction during the spring response time. However, this needs the simulations in the bare hull and self-propulsion conditions to reach an ideally converged state with very small and constant oscillations of the ship instantaneous velocity and surge motion and hence spring and light-weight carriage forces. Moreover, the derivation of the instantaneous thrust deduction factor requires exactly identical instantaneous ship velocity during the spring response time in bare hull and self-propulsion conditions, because even small velocity variations result in significant resistance and thrust change, and consequently, alterations of the spring and light-weight carriage forces. Therefore, the instantaneous thrust deduction factor and wake fraction cannot be achieved in the investigations in Paper V. Instead, the averaged thrust deduction factor, wake fraction and other aforementioned propulsive factors can be obtained according to the averaged values of different quantities during a time window, for instance roughly on one spring natural period T_{spring}, on which the averaged velocity of the ship remains very close to the expected ship velocity U.

In each model SPP condition, it is required to have a propeller rotational speed that yields a zero mean surge motion (from the generated propeller thrust) during the ship performance at the intended ship velocity. However, it is extremely time-consuming and computationally expensive to find the precise propeller rotational speed at the self-propulsion point of the model (which yields precisely zero mean surge) in the RANS investigations, especially in regular head waves. Therefore, an estimated propeller rotational speed at the model SPP is adopted in the simulation in each condition in Paper V to yield a near-to-zero surge motion. However, based on the accuracy of such estimation in each operational condition, the spring system response might vary, resulting in small (but not negligible) mean surge motion and acceleration and hence operating in a self-propulsion point very close, but not identical, to the self-propulsion point of the model (model SPP). Consequently, in Paper V, the eventual spring and light-weight carriage forces, retained in the simulations and originated from the surge motion and acceleration with regards to the generated thrust in the adopted propeller rotational speeds, are considered as external forces to adjust the force imbalance to reach the self-propulsion point of the model at the desired ship forward velocity U.

Therefore, the mean thrust deduction factor $\bar{t}$ is estimated using mean values (during the chosen time window) of total resistance $\bar{R}_T^{BH}$ from the bare hull simulation results in Paper III together with the propeller thrust $\bar{T}^{SP}$ as well as the spring force $-K\bar{x}^{SP}$ and light-weight carriage force $-m_3\bar{\ddot{x}}^{SP}$ from the self-propulsion simulation results in Paper V. The mean value of the ship velocity during the same time window remains very close to U in both bare hull and self-propulsion conditions, which justifies the derivation of the mean thrust deduction factor in that velocity through,

$$\bar{t} = 1 - \frac{\bar{R}_T^{BH}}{\bar{T}^{SP} + (-K\bar{x}^{SP} - m_3\bar{\ddot{x}}^{SP})}, \tag{2.31}$$

in which $(-K\bar{x}^{SP} - m_3\bar{\ddot{x}}^{SP})$ represents the additional force that compensates for the propeller thrust deficit/excess in self-propulsion condition at the estimated propeller rotational speed to reach model SPP. It should be noted that this additional force $(-K\bar{x}^{SP} - m_3\bar{\ddot{x}}^{SP})$ does not influence the flow physics in the same way as the propeller thrust generation mechanism, and its consideration in Paper V is related to the correction of the thrust deficit/excess at the estimated propeller rotational speed. The corrected thrust, eventually, is used for the estimation of the thrust deduction factor. However, since the spring and light-weight carriage forces are relatively insignificant, their effects on the main analyses carried out in this thesis are deemed inconsequential.

2.4.1 Self-propulsion in Calm Water

The propeller rotational speed n^{SP}, propeller thrust T^{SP} and propeller torque Q^{SP} can be derived from the experimental and numerical self-propulsion investigations in calm water. Then the mean thrust deduction and wake fraction as well as the other aforementioned propulsive characteristics can be calculated in model-scale.

2.4.2 Self-propulsion in Regular Head Waves

ITTC (2021e) describes two techniques for model guidance in self-propulsion model tests in regular head waves: captive and free-running. In the former, the model is connected to the carriage by a force gauge and the speed is controlled by the towing carriage, hence the measured force corresponds to the self-propulsion point. In free-running conditions, the model is auto-piloted and speed-controlled, hence the self-propulsion point is derived through the averaged speed monitored by a tracking system.

In Paper V, the self-propulsion studies concern the ship free in 3DOF by means of a weak spring system. In the simulation in each wave condition, a propeller rotational speed that yields a near-to-zero mean surge motion is estimated to reach the model SPP. However, in the experiments, the chosen propeller rotational speed in each wave condition does not necessarily match the considered propeller speed at the model SPP in the numerical method. Consequently, the CFD investigations in Paper V are divided into two categories: one focusing on the validation practice by considering similar propeller rotational speed as in model tests, and another for the analysis of the propeller-hull interaction effects by adopting the estimated propeller rotational speeds at the model SPP.

From the bare hull results in Paper III and the self-propulsion results in Paper V in regular head waves, the mean thrust deduction and wake fraction as well as the other aforementioned propulsive factors are calculated and compared to those of calm water. The mean wake fraction is estimated by the thrust

identity method based on the propeller open water curves, derived in Paper IV and explained in Section 2.3.

In Paper I, the FNPF mean wave making resistance $\bar{R}_W^{BH}$ of the bare hull in regular head waves are compared to the free-running self-propulsion experimental mean wave making resistance $\bar{R}_W^{SP}$ estimated from the mean thrust in regular head waves $\bar{T}^{SP}$ as,

$$\bar{R}_W^{SP} = (1 - \bar{t})\bar{T}^{SP} - (1 + k)\bar{R}_F, \tag{2.32}$$

in which $\bar{t}$ in regular head waves is assumed to be identical to the calm water value at the same ship speed. Furthermore, since the model was running in free-sailing self-propulsion mode, the mean value of the measured speed $\bar{U}$ was not exactly equal to the expected U. The Reynolds number in Equation 2.5 and accordingly C_F in Equation 2.4 are calculated for the mean attained speed $\bar{U}$. Then $\bar{R}_F$ in waves is calculated assuming the same wetted surface area and hence similar frictional resistance in waves as in calm water at each certain ship speed. These assumptions are examined in Paper III and Paper V using RANS-based numerical simulation.

Chapter 3

Summary of Appended Papers

In this chapter, the summaries of the five appended papers are provided.

3.1 Paper I

"Investigation of ship responses in regular head waves through a Fully Nonlinear Potential Flow approach". Irannezhad, M., Eslamdoost, A., Kjellberg, M., and Bensow, R. E. (2022a). *Ocean Engineering* 246. https://doi.org/10.1016/j.oceaneng.2021.110410

CRediT Authorship Contribution Statement

Mohsen Irannezhad: Conceptualization, Formal analysis, Investigation, Data curation, Writing – original draft, Writing – review & editing, Visualization. **Arash Eslamdoost**: Conceptualization, Resources, Writing – original draft, Writing – review & editing, Supervision, Project administration, Funding acquisition. **Martin Kjellberg**: Methodology, Writing – review & editing, Supervision. **Rickard E. Bensow**: Conceptualization, Resources, Writing – review & editing, Supervision, Project administration, Funding acquisition.

Scope and Objectives

Paper I presents the first step towards the investigations of the propeller-hull interaction effects in calm water and regular head waves, explained in Section 1.4, through the analysis of a bare hull performance using a Fully Nonlinear Potential Flow (FNPF) panel method. The main objective was to study the overall hydrodynamic performance of a general cargo vessel bare hull in a broad range of operational conditions, i.e., loading conditions, ship velocities, wave heights and wave lengths, in model-scale and free in 3DOF in calm water and

regular head waves by analyzing the ship motions and their correlation with the wave making resistance.

The computational results were compared to the available experimental data from the Maritime Research Institute Netherlands (MARIN). The model tests resistance data in calm water concerned the bare hull, whereas in regular head waves, the results of the free-running self-propulsion (6DOF) model tests were used. The mean wave making resistance in regular head waves was estimated from the mean propeller thrust measured in the self-propulsion tests, based on the assumption of equal thrust deduction and mean frictional resistance in calm water and regular head waves, as explained in Section 2.4.2.

Two loading conditions were considered, namely, fully-loaded and ballast. The investigations in calm water at different ship speeds include resistance simulations as well as free decay heave and pitch simulations with different degrees of freedom for obtaining natural periods of these motions. On the other hand, a wide range of wave conditions (lengths and heights) were considered for the investigations in regular head waves, in which the Fourier analysis was carried out and the dominant harmonic amplitudes of motions and resistance were analyzed.

Results and Conclusions

Calm Water

The computed wave making resistance and motions by the FNPF method in calm water were in rather good agreement with the experimental data. It was seen that the motion coupling slightly increases both heave and pitch natural periods, which may reflect the importance of motion coupling in the ship performance evaluation.

Regular Head Waves - Motions

The 1st harmonic amplitudes of motions were the dominant components in the Fourier analysis performed in regular head waves. The 2nd harmonic amplitudes of motions were significantly lower than the 1st harmonic amplitudes, except in very short waves where both components were small and the ship motion responses were nonlinear with very small magnitudes.

In both loading conditions, the 1st harmonic amplitudes of heave motion z_1, when plotted versus wave encounter frequency, exhibited local maxima near the heave resonance conditions, i.e., when the encounter wave frequency was close to the heave natural frequency. The local maxima near the resonance conditions were seen in the 1st harmonic amplitudes of pitch motion θ_1 solely in the ballast condition, whereas in the fully-loaded condition, the increasing pitch excitation wave forces near resonance conditions were believed to be the main reason for the absence of local maxima. On the other hand, θ_1 exhibited large peaks resulting from high excitation wave forces near $\lambda/L = 1.24$ and $\lambda/L = 1.35$ in the fully-loaded and ballast conditions, respectively. Furthermore, secondary local maxima for θ_1 were seen near $\lambda/L = 0.55$ in both loading conditions.

The 1st harmonic phase differences between heave and pitch motions $z_{\varepsilon 1} - \theta_{\varepsilon 1}$ versus wave length exhibited rather similar trends in different operational conditions. Interesting abrupt transitions were seen in the phase difference curves near $\lambda/L = 0.55$.

Regular Head Waves - Resistance

In each loading condition, the plot of added wave resistance coefficient C_{AW} versus wave length exhibited two peaks, roughly in $\lambda/L \approx 0.5$ and $\lambda/L \approx 1.0$. Although in the fully-loaded condition the peak in the longer wave was dominating and it coincided with resonance, the peaks were rather equal in size in the ballast condition. It was believed that these secondary peaks in the shorter wave were related to the secondary peaks of θ_1 as well as the abrupt transitions of the 1st harmonic phase difference between heave and pitch motions observed near such wave lengths.

Final Remarks

Although the computed motions in the FNPF method were comparable to the measurements, the resistance results were arguably less accurate in some conditions. The averaged absolute error of FNPF computational results in terms of percentage of the experimental values in both loading conditions for surge, heave and pitch 1st harmonic amplitudes were 34.6%, 19.6% and 17.1%, respectively. When the effects of actual measured wave height in the model tests were taken into account, the average absolute error of the non-dimensional 1st harmonic amplitudes of surge, heave and pitch motions reduced to 26.2%, 18.1% and 11.8%, respectively. On the other hand, the averaged absolute errors associated with the mean wave making resistance and added wave resistance coefficient (considering the actual incident wave height in the experiments) were found to be 25.0% and 24.3%, respectively.

Generally, numerical errors in conjunction with the discretization errors as well as the potential flow approximations and the use of empirical formulas, such as the ITTC-57 model-ship correlation line, were the main sources which contributed to the discrepancy between the computed and the measured results. Moreover, the uncertainty related to the experimental data as well as the differences between the experimental and numerical setups (6DOF self-propelled against 3DOF bare hull) in this paper should not be forgotten. The frictional resistance and thrust deduction factor in waves were assumed to be equal to those of calm water. However, the interaction effects between waves, hull and propulsion system may dispute the validity of these assumptions, hence introducing additional sources of discrepancy between FNPF and EFD.

The change of the mean wetted surface area, derived from averaging the wetted surface area over an encounter wave period, remained mainly less than 1% of the calm water wetted surface area. Based on a simple approximation in the FNPF solver, the change of the frictional resistance in the presence of waves was found to be less than 2% of the respective calm water values. This approximation did not take into account the viscous effects, such as periodic flow separations at the stern, splashes, bow and stern slamming and green

water on deck, and solely relied on the ITTC-57 model-ship correlation line for the estimation of frictional resistance. Supplementary investigations on the change of thrust deduction factor as well as frictional resistance in the presence of waves by higher fidelity viscous flow methods were encouraged in this paper, leading to one of the main objectives of this thesis and hence investigated in the other appended papers.

Comments

The FNPF computational cost for each simulation was approximately $20 - 80$ core-hours which lies between the computational cost required by lower fidelity methods (often with lower accuracy) such as methods based on Strip Theory and higher fidelity methods such as viscous flow solvers. This was mainly discussed in Publication B, Irannezhad et al. (2019b), but since it is not directly related to the thesis objectives, it is not appended in the thesis. The utilization of the FNPF methods in the prediction of the overall performance of ships in regular head waves in terms of ship motions and resistance was found to be computationally efficient and cost-effective. However, given that the bare hull performance investigations include nominal wake analysis in conjunction with ship motions and resistance, the utilization of a viscous flow method for the evaluation of the hull hydrodynamic performance in calm water and regular head waves was motivated. Therefore, RANS investigations were conducted extensively in the other appended papers in this thesis.

One important point is that in the subsequent papers, the RANS investigations concerned another ship (KVLCC2 tanker) mainly because of the availability of extensive model test data for this ship, especially the SPIV wake measurements which are rather scarce. Nonetheless, the obtained knowledge in Paper I regarding the correlations between different ship motions and wave making resistance facilitates the analysis of the RANS investigations in the following papers.

3.2 Paper II

"Towards uncertainty analysis of CFD simulation of ship responses in regular head waves". Irannezhad, M., Bensow, R. E., Kjellberg, M., and Eslamdoost, A. (2021). *Proceedings of the 23rd Numerical Towing Tank Symposium (NuTTS 2021)*, pp. 37–42. https://www.uni-due.de/imperia/md/content/ist/nutts_23_2021_mulheim.pdf

CRediT Authorship Contribution Statement

Mohsen Irannezhad: Conceptualization, Formal analysis, Investigation, Data curation, Writing – original draft, Writing – review & editing, Visualization. **Rickard E. Bensow**: Conceptualization, Writing – review & editing, Supervision. **Martin Kjellberg**: Conceptualization, Writing – review & editing,

Supervision. **Arash Eslamdoost**: Conceptualization, Resources, Writing – review & editing, Supervision, Project administration, Funding acquisition.

Scope and Motivations

Paper II presents an important intermediate step towards the RANS investigations of ship performance in regular head waves. In this paper, the numerical wave propagation in an empty computational domain (without the presence of the hull) was thoroughly studied. The aim was to achieve a robust wave propagation simulation setup and minimize the modeling errors of wave propagation, e.g., amplitude reduction and period change during propagation, disturbances (wiggles) on the free surface and reflection at boundaries. The obtained numerical waves were compared to the analytical waves and the discrepancies were discussed.

In order to be consistent with the bare hull, POW and self-propulsion RANS investigations in Paper III - Paper V, the considered wave conditions in Paper II were chosen to represent the wave conditions under which the operational performance of the KVLCC2 was analyzed. These conditions particularly involved three regular head waves, all with the same wave height $H/L = 0.01875$ and three different wave lengths $\lambda/L = 0.6$, 1.1 and 1.6. It was presumed that the steepest wave was the most critical wave for numerical propagation modeling, hence the wave with $\lambda/L = 0.6$ was chosen to perform the investigations in Paper II.

The computational domain in the ship performance investigations in Paper III and Paper V discretized employing an Overset Topology consisting an overset region and a background region with specific treatment of cell sizes near the overlapping zone (where the information is exchanged between the background and overset regions). In order to take into account various aspects of numerical wave modeling in Paper II, four different grid sets were studied with different local refinement zones and overset motion considerations. In each grid set, four systematically refined unstructured grids were considered which were determined by the refinement levels $n = 0.50$ (coarsest), 1.00, 1.50 and 2.00 (finest). The wave elevation was analyzed at 16 wave probes within the computational domain and the Fourier analysis was carried out to derive the harmonic amplitudes of wave elevation monitored in each probe. Consequently, the effects of different local refinement zones as well as the quality of the cell size and overset interpolations in the overlapping zones were evaluated.

Results and Conclusions

A robust simulation setup for wave propagation in the employed RANS solver was achieved, in which the quality of the numerical waves was improved through various attempts. The propagating numerical waves from the simulations were rather comparable to the analytical waves and the discrepancies remained relatively low for different grids, except the coarsest grid $n = 0.50$. The coarsest

grid was found to be incapable of capturing the main flow features as the results of the grid significantly deviated from those of the other grids.

Overall, the numerical configuration proposed in this paper yielded numerical waves that closely resembled the theoretical counterpart, with discrepancies in the 1st harmonic amplitude (i.e., the dominant component) remaining mainly below 3% for the grids $n = 1.00$, 1.50 and 2.00.

Comments

It should be mentioned that, in this paper, the preliminary RANS investigation of bare hull performance in regular head waves was also briefly presented. Nevertheless, these investigations were further developed in Paper III, hence the preliminary results obtained in Paper II are not discussed here, instead the matured results are discussed under the summary of Paper III.

3.3 Paper III

"Comprehensive computational analysis of the impact of regular head waves on ship bare hull performance". Irannezhad, M., Bensow, R. E., Kjellberg, M., and Eslamdoost, A. (2023). *Ocean Engineering* 288. https://doi.org/10.1016/j.oceaneng.2023.116049

CRediT Authorship Contribution Statement

Mohsen Irannezhad: Conceptualization, Formal analysis, Investigation, Data curation, Writing – original draft, Writing – review & editing, Visualization. **Rickard E. Bensow**: Conceptualization, Writing – review & editing, Supervision. **Martin Kjellberg**: Conceptualization, Writing – review & editing, Supervision. **Arash Eslamdoost**: Conceptualization, Resources, Writing – original draft, Writing – review & editing, Supervision, Project administration, Funding acquisition.

Scope and Motivations

Paper III demonstrates the first step towards the investigations of the propeller-hull interaction effects in calm water and regular head waves, illustrated in Section 1.4, through the analysis of a bare hull performance using a RANS solver. In this paper, in addition to the ship motions and resistance, the nominal wake of the KVLCC2 bare hull in model-scale with a scale factor of 100 ($L = 3.2$ m) was examined. The investigations concerned four operational conditions all at the design Froude number $Fr = 0.142$ ($U \approx 0.797$ m/s) and in the design loading condition while being free to surge, heave and pitch (3DOF): one in calm water and three in regular head waves with the same wave height $H/L = 0.01875$ and three different wave lengths $\lambda/L = 0.6$, 1.1 and 1.6.

The main objective was to identify the impact of regular head waves on the bare hull resistance, motions and nominal wake as well as the correlations

between them, in comparison to calm water condition. The correlations between the wake variations and the ship motions as well as the possible consequential effects on the propeller loading considering both the wake and resistance during the bare hull performance in regular head waves were investigated.

The available experimental data from Osaka University Towing Tank were used for validation of the computational results. The model test setup concerned the hull free to surge while it was towed with a light-weight carriage connected to the main carriage through a weak spring system (spring stiffness $K = 98$ N/m). An external constant towing force F_0 (obtained through a set of preliminary tests) was exerted in each model test in order to keep the calm water surge and the mean surge in waves close to zero and hence restrict large compression/expansion of the spring. Unfortunately, F_0 was not available from the model test data.

In the simulations, the effects of spring and F_0 were replicated by exerting external forces at the ship COG in the ship advancing direction. However, an estimated F_0 was considered in the simulations in each operational condition, due to the lack of information from the model tests. The convergence of simulations was examined based on suitable convergence criteria defined on the ship resistance in each operational condition, while using a carefully defined time window for the Fourier analysis and post-processing of the results in order to include the spring effects.

The nominal wake measurements (SPIV) were performed on a plane fixed on the carriage, so the hull moved around the original position of the plane with the wave encounter frequency and the spring natural frequency. The carriage-fixed wake computations were compared to those of SPIV measurements, and then the hull-fixed nominal wake from simulations were analyzed thoroughly.

Three velocity components of the nominal wake (i.e., axial u, transversal v and vertical w) were time-averaged ($\bar{u}$, $\bar{v}$, $\bar{w}$) and/or surface-averaged ($\tilde{u}$, $\tilde{v}$, $\tilde{w}$) in distinct ways in order to extract and present the main features of the flow. The surface-averaged wake concerned the averaging over the whole propeller disk as well as the circumferential-averaged wake. The time-averaging was carried out in three ways: for each extracted data point on the propeller disk surface area, for the circumferential-averaged wake at different radii, or for the surface-averaged wake over the whole propeller disk giving $\bar{\tilde{u}}$, $\bar{\tilde{v}}$ and $\bar{\tilde{w}}$).

A grid convergence study was carried out employing a numerical uncertainty analysis tool developed by Eça and Hoekstra (2014) and Eça et al. (2019) based on the Least Squares fits to power series expansions. The same grids were used for the simulations in calm water and regular head waves. In the grid convergence study, five systematically refined "as geometrically similar as possible" unstructured grids were generated which were determined by the refinement levels $n = 0.75$ (coarsest), 1.00, 1.25, 1.50 and 2.00 (finest). The results of an additional coarser grid with refinement level $n = 0.50$ were excluded as it was found that such grid was incapable of capturing the main flow features and yielding drastically lower quality numerical waves, as discussed in the summary of Paper II.

Results and Conclusions

Carriage-fixed Wake Validation

A reasonably good agreement was seen for the qualitative wake comparisons between CFD wake and EFD SPIV measurements. The potential sources of discrepancies, particularly the difference between the considered F_0 and hence inconsistency of spring behavior and surge motion were explained. Moreover, the uncertainties related to the exact time instances of wake measurements were also addressed.

Calm Water - V&V

Although the grid convergence study for the calm water resistance showed rather large numerical uncertainties (8.8% to 14.9%), the computed resistance from different grids were similar in terms of magnitude. The large numerical uncertainties were, in part, attributed to the curve fitting method used in the employed numerical uncertainty analysis technique. It was suggested that a linear curve fitting could have been a more practical alternative than the second-order method in the employed uncertainty analysis tool. The computed resistance and motions in calm water were in rather good agreement with the measured data, especially when the discrepancies were compared in terms of magnitude with respect to the accuracy of the computations and measurements.

For the axial velocity component of the nominal wake on the hull-fixed propeller disk $\bar{\tilde{u}}$ in calm water, the numerical uncertainties were higher (18.1% to 31.0%) than those of resistance. Contrary to the motions and resistance, significant differences of $\bar{\tilde{u}}$ were seen between different grids, which in conjunction with the high uncertainties, indicated the importance of grid refinement for the wake predictions. Moreover, significant differences in the magnitude and profile of the circumferential-averaged axial wake were observed between different grids, especially in the radius of $0.6 < r/R < 0.8$ (R is the propeller radius) where often a substantial part of the propeller thrust is generated. Therefore, significantly different wake-adapted propeller designs can be proposed depending on the choice of the grid in calm water.

Regular Head Waves - V&V

The numerical uncertainties for the 1st harmonic amplitudes of the heave and pitch motions were relatively lower (0.7% to 8.2%) than the numerical uncertainties of the mean total resistance (6.6% to 11.1%). However, since the results of different grids were very similar in terms of magnitude, a linear line might be a better candidate for curve fitting for these quantities, similar to the calm water resistance.

The averaged absolute error $\overline{|E\%D|}$, computed from averaging the absolute errors of the mean total resistance and the 1st harmonic amplitudes of surge, heave and pitch motions, for the simulations in $\lambda/L = 1.1$ and 1.6 with the grid $n = 1.00$ in comparison to EFD were approximately 10.4% in dimensional quantities but 7.4% in the non-dimensional ones, whereas increased from 8.3% to

12.4% in $\lambda/L = 0.6$. This increase was justified by considering the insignificant magnitudes of the 1st harmonic amplitudes of motions, and hence derivation of large errors as a consequence of small discrepancies, as well as considering the significance of the higher harmonic amplitudes compared to the 1st harmonic amplitude in such short waves. This was also discussed in Paper I that in short waves the higher harmonic amplitudes can become significantly important and the ship motions were nonlinear with very small magnitudes.

In regular head waves, the numerical uncertainties of the mean axial velocity of wake were relatively higher (4.9% to 32.1%) than that of mean total resistance and the 1st harmonic amplitudes of motions, similar to the calm water condition.

Hydrodynamic Performance - Resistance and Motions

Although the behavior of heave and pitch motions during one encounter period, observed through the analysis of reconstructed time series, was completely different in different wave lengths, the behavior of total resistance was roughly similar for all three waves, with minimum/maximum values occurring approximately when the wave trough/crest is close to the ship fore perpendicular. Larger variations were seen for the total resistance during one encounter period in $\lambda/L = 0.6$ and 1.6 in comparison to $\lambda/L = 1.1$, while the mean total resistance was higher in $\lambda/L = 1.1$ mainly due to the effects of higher harmonic amplitudes in this wave length. Therefore, a self-propelled hull in $\lambda/L = 1.1$ has to deliver a larger average thrust in comparison to the other wave lengths, but the load variation and consequently the maximum and minimum loading conditions on the propeller will be more severe in the shorter and longer wave lengths. Such load variations can impose several design constraints both for the propeller and the machinery system.

The contribution of the added shear resistance on the total added resistance of the hull was 6.8%, 2.9% and 4.6% for the shortest wave to the longest one in grid $n = 1.00$, which was relatively small but not negligible. Moreover, it was found that the time-averaged wetted surface area in waves was almost equal to that of calm water. Therefore, it is concluded that the viscous phenomena such as increased turbulence by the wave orbital velocities contribute to the increased frictional resistance in waves relative to calm water. Consequently, the conventional frictional resistance prediction methods, such as the ITTC-57 model-ship correlation line, cannot be directly used for the frictional resistance prediction in waves. This actually disputes one of the assumptions considered in Paper I and might introduce an extra source of discrepancy between the EFD data and FNPF results in this paper.

Hydrodynamic Performance - Nominal Wake

The variation of nominal wake in waves could be associated with the instantaneous propeller disk velocities, boundary layer contraction/expansion due to hull motions, bilge vortex dynamics, shaft vortex dynamics and the orbital wave velocities at the propeller disk as well as the complex interactions between these factors in different operational conditions. During one encountered wave period in regular head waves, quite significant variations were seen for

the axial velocity component of the wake and the time-averaged values in all three waves were larger (approximately 9.8%, 21.3% and 14.6% for $\lambda/L = 0.6$, 1.1 and 1.6, respectively) than the calm water value. The variations in the transversal velocity components remained insignificant in terms of magnitude in comparison to the axial component. However, large variations were seen for the vertical velocity component, similar to the axial component. The trend of the wake velocities during one encounter wave period was different in different wave lengths, while the resistance trends were rather similar. Therefore, the expected propeller thrust in self-propulsion undergoes different alterations over time than the required thrust to overcome the resistance in different wave lengths, which may introduce significant propeller design constraints.

In $\lambda/L = 0.6$, due to small ship motions, the variation of wake during one encounter wave period from its time-averaged value was found to be mainly affected by the wave orbital velocities. However, in $\lambda/L = 1.1$ and 1.6 the ship motions introduced significant effects on the flow physics, and different factors were found to contribute to the transient wake. Overall, the large hull motions in the longer waves dictated the variation of wake through the contraction/expansion of the boundary layer as well as imposing vortical structure dynamics. However, the wave orbital velocities were the dominant factor in the shortest wave where the hull motions were insignificant.

The contour plots of the time-averaged wake difference between the waves and the calm water conditions showed the regions with velocity deficit and excess in waves relative to calm water. These results in $\lambda/L = 1.1$ and 1.6 pinpointed the missing bilge vortex and the secondary shaft vortex in comparison to the calm water wake. Since a propeller is often designed based on the calm water nominal wake, any deviation from the calm water wake alters the loading distribution on the blade resulting in an adverse effect on the propeller performance.

Significant variations were seen for the circumferential-averaged axial velocity of wake during one encountered wave period in the regular head waves simulations, especially in $\lambda/L = 1.1$ and 1.6 where the motions are large. Such variations were significant near the propeller tip which might impact the local blade loading, the dynamics of the tip vortex, and the cavitation pattern on the blades. The time-average of the circumferential-averaged axial velocity of wake showed a rather similar radial distribution in $\lambda/L = 0.6$ in comparison to calm water, while being noticeably different in $\lambda/L = 1.1$ and 1.6, especially between $0.282 < r/R < 0.704$, where a significant proportion of the propeller thrust is often generated. Although the time-average of the circumferential-averaged vertical velocity of the wake was rather similar in waves and calm water, the variations during one encounter wave period were significant, which might be important for the angle of attack and hence propeller design.

Final Remarks

The paper revealed a substantial dependency of the wake on grid resolution, particularly in calm water and shorter waves, while motions and resistance indicated a weaker dependency. This means that although rather reliable

resistance and motion predictions could be derived from the coarser grids, the nominal wake predictions were significantly dependent on the choice of the grid. This dependency was stronger in calm water and the shortest wave $\lambda/L = 0.6$, in which the hull motions and hence bilge vortex dynamics were insignificant and the numerical uncertainties were mainly imposed by the accuracy of the predicted flow-driven phenomena such as the budging bilge vortex. On the other hand, the grid refinement dependencies and numerical uncertainties were lower for the longer waves in which significant vortex dynamics were observed due to the large hull motions and the accuracy of the predicted wake was mainly governed by the ship dynamics.

Comments

Although the finer grids mainly exhibited superior results, particularly for the nominal wake predictions, the computational costs associated with such grids were relatively high. Hence, the choice of the refinement level heavily depends on the available computing resources. A very rough estimation of the total computational costs used for the simulations in calm water and in regular head waves of $\lambda/L = 1.1$ both with grid $n = 1.00$ was approximately 22000 and 25000 core-hours, respectively. These were several orders of magnitude larger than the computational costs involved in the FNPF method in Paper I. However, the accuracy of the results was rather high in the employed RANS solver. Moreover, the flow field analyses in the RANS solver provided valuable insight into the hull-wave interaction effects and contributed to the comprehension of the underlying physical mechanisms, which was not feasible through the FNPF method.

3.4 Paper IV

"Experimental and numerical investigations of propeller open water characteristics in calm water and regular head waves". Irannezhad, M., Kjellberg, M., Bensow, R. E., and Eslamdoost, A. (2024a). *Preprint Under Review in Ocean Engineering, available at SSRN.* http://doi.org/10.2139/ssrn.4706213

CRediT Authorship Contribution Statement

Mohsen Irannezhad: Conceptualization, Formal Analysis, Investigation, Data Curation, Writing – Original Draft, Writing – Review & Editing, Visualization. **Martin Kjellberg**: Conceptualization, Writing – Review & Editing, Supervision. **Rickard E. Bensow**: Conceptualization, Writing – Review & Editing, Supervision. **Arash Eslamdoost**: Conceptualization, Resources, Writing – Original Draft, Writing – Review & Editing, Supervision, Project Administration, Funding Acquisition.

Scope and Motivations

Paper IV covers the second step towards the investigations of the propeller-hull interaction effects in calm water and regular head waves, explained in Section 1.4, through the analysis of POW performance using model tests as well as a RANS solver. In this paper, the open water characteristics of the KVLCC2 propeller (KP458) in model-scale with a scale factor of ≈ 45.714 (diameter of $D = 0.2157$ m) were examined. The propeller open water model tests were carried out at the SSPA towing tank. It is worth mentioning that the scale factor in this paper is different from the considered scale factor in Paper III, due to the availability of the model propeller at SSPA for the measurements.

The main objective was to study the impacts of regular head waves on the open water characteristics of a fully-submerged non-ventilating propeller and analyze the associated flow physics. The intention was to perform the POW performance evaluation of the propeller in calm water and regular head waves under a similar operational condition as the propeller experiences behind the self-propelled KVLCC2 at its design Froude number, but without accounting for the propeller interaction effects with the hull. The investigations mainly concerned four advance ratios of the propeller, i.e., $J \approx 0.35$, 0.45, 0.55 and 0.60, derived from a constant advance velocity (carriage speed) and varying the propeller rotational speed. The considered advance velocity $U \approx 1.177$ m/s represents the design speed of KVLCC2 at the same scale factor as that of the propeller. Consequently, the advance velocity in this paper is different from the advance velocity considered in Paper III, nonetheless representing the same Froude number of KVLCC2 (design Froude number $Fr = 0.142$).

In Paper III, for the scale factor of 100 ($L = 3.2$ m), the three studied waves had the same wave height $H/L = 0.01875$ and three different wave lengths $\lambda/L = 0.6$, 1.1 and 1.6, hence the steepness of $H/\lambda \approx 3.125\%$, 1.705% and 1.172%, respectively. In Paper IV, the scale factor was ≈ 45.714 ($L = 7$ m) and the generation of high-quality waves with the length of $\lambda/L = 1.6$ was not only restricted by the wave maker capacity but also in such very long waves and the high carriage speed, the number of encountered waves was limited in each carriage run. On the other hand, before the start of the POW investigations in Paper IV, the wave steepness was deemed to be the key factor affecting the propeller open water characteristics in regular head waves. Therefore, the initial plans were made in order to aim for POW investigations in similar wave steepness as those considered in Paper III, but taking into account only the wave lengths $\lambda/L = 0.6$, 1.1 with different wave heights. However, according to the wave propagation calibration tests in the empty tank (prior to the POW tests), the generation of these waves with high quality was also restricted by the wave maker capacity. As a result, the intended waves from the calibration tests included three wave conditions in $\lambda/L = 0.57$ with three different wave heights resulting in steepness of $H/\lambda \approx 1.052\%$, 1.754% and 3.007% (WC1-WC3), as well as one wave condition in $\lambda/L = 1.078$ with a wave height resulting in steepness of $H/\lambda \approx 1.762\%$ (WC4). Overall, five environmental conditions were considered: one in calm water and four in regular head waves with different wave lengths and heights (WC1 to WC4) primarily with the submergence depth

of $3R$ to avoid propeller ventilation so the wave effects is not influenced by the propeller ventilation.

The propeller Reynolds number in the towing tank tests was approximately between 2.03×10^5 and 3.38×10^5, which is just above the minimum Reynolds number for POW test by the ITTC. Therefore, the effect of transition from laminar to turbulent flow was also studied in the CFD investigations.

The convergence of simulations was examined based on different criteria defined on the propeller thrust and torque in each operational condition using a carefully defined time window for the post-processing of the results. A formal verification and validation (V&V) procedure was also used to assess the numerical uncertainty of the CFD result.

The investigations involved analyzing instantaneous, time-averaged, and harmonic amplitudes of propeller thrust, torque, and efficiency, along with single-blade load variations and an incident flow field analysis from CFD simulations.

Results and Conclusions

Calm Water - V&V

The conducted calm water towing tank tests in conjunction with the performed simulations incorporating the $\gamma - Re_\theta$ transition model TM and the fully turbulent simulations FT (without transition model) revealed the existence of laminar to turbulence transition.

Overall, the open water characteristics of the propeller in calm water derived from the TM simulations agreed better than the FT simulations when compared to the EFD results. The validation errors are lower for the TM simulations, especially at higher advance ratios. The averaged absolute error $\overline{|E\%D|}$, computed by taking the average of the absolute errors in all advance ratios in calm water, was reduced from FT to TM simulations: approximately from 2.8% to 1.4% for thrust coefficient, from 7.3% to 1.7% for torque coefficient and from 7.6% to 3.1% for propeller efficiency.

The grid convergence study from the TM simulations at $J \approx 0.55$ in calm water resulted in numerical uncertainties approximately between 6% and 8% for both thrust coefficient K_T and torque coefficient K_Q, but smaller $1 - 4\%$ for the propeller open water efficiency η_O.

Regular Head Waves - V&V

The reconstructed time series of K_T, K_Q and η_O were decreasing/increasing depending on whether the analytical wave crest or trough is located at the propeller disk. In the wave crest the wave orbital velocity in the axial direction becomes maximum, thus resulting in an increased temporal advance ratio and consequently decreased propeller loading. The opposite holds for the wave trough. This can be perceived by considering the open water curves for K_T and K_Q in calm water and taking into account the temporal changes in advance ratio. However, in contrast to the calm water efficiency, the reconstructed time

series of η_O exhibited a similar trend as of K_T and K_Q in waves, independent of the advance ratio. This behavior cannot be fully explained by solely relying on the temporal advance velocity change, however, it was found that the dynamics of the geometric advance angle explain the variations of thrust and torque as well as the propeller efficiency in waves.

Based on the results from FT and TM simulations as well as the clear change of propeller characteristics from EFD in waves in comparison to calm water, it was concluded that the aforementioned laminar flow dominance in calm water, may not persist in the case of regular head waves. The reason might lie in the complex dynamics of the incident flow in waves as well as the presumably higher turbulence level generated by the wave maker in the towing tank. Therefore, the TM simulation results in calm water and the FT simulation results in waves were analyzed to understand the impact of waves on the POW performance through the employed CFD approach.

In both EFD and CFD, the 0th harmonic amplitudes of K_T, K_Q and η_O (i.e., $\bar{K}_T$, $\bar{K}_Q$ and $\bar{\eta}_O$) in all of the considered waves were clustered at each corresponding advance ratio. Therefore, it can be concluded that, a similar effect across different wave conditions was seen at each advance ratio. The largest discrepancies of the 0th harmonic amplitudes between CFD and EFD were seen for $\bar{K}_T$ and $\bar{K}_Q$ at the higher advance ratios $J \approx 0.55$ and 0.60, while $\bar{\eta}_O$ as the correlation between thrust and torque coefficients was agreed better. The averaged absolute error for $\bar{K}_T$, $\bar{K}_Q$ and $\bar{\eta}_O$ in all of the wave conditions and advance ratios were 6.3%, 4.2% and 2.3%, respectively, which are higher than the calm water values for thrust and torque, but slightly lower for efficiency.

In both EFD and CFD, the 1st harmonic amplitudes of K_T, K_Q and η_O (i.e., K_{T1}, K_{Q_1} and η_{O1}) were increasing at higher advance ratios in the same wave condition. This may be related to the fact that in the higher advance ratios the propeller rotational speed is lower, hence the effects of the axial component of the wave orbital velocities become more significant on the advance ratio. Overall, K_{T1}, K_{Q_1} and η_{O1} were mainly under-predicted by CFD in comparison to EFD and the averaged absolute errors were smaller (2.7% and 4.2%) for the thrust and torque coefficients but very significant (14.8%) for efficiency.

The grid convergence study from the FT simulations in WC2 at $J \approx 0.55$ resulted in numerical uncertainties approximately $0.9-2.8\%$ for $\bar{K}_T$, $2.9-8.4\%$ for $\bar{K}_Q$, and $0.7-1.1\%$ for $\bar{\eta}_O$, which were mainly lower than calm water values. Substantially larger numerical uncertainties were seen for K_{T1}, K_{Q_1} and η_{O1}, especially for K_{Q_1} and η_{O1} $(36.6-42.9\%)$.

Final Remarks

In this study, the CFD results demonstrated promising agreement with experimental measurements, highlighting the inherent unsteady and non-uniform oblique flow effects of propagating regular waves. Analyses of the incident flow field, including the geometric advance angle and wave orbital velocities, alongside single-blade force and moment investigations, reveal potential sources

of discrepancies between EFD and CFD data. Asymmetric conditions and mechanical interference in experiments, absent in the ideal conditions in CFD, are identified as factors influencing flow dynamics, transition, separation, and vortical structures formation. The study highlights the shortcomings of RANS and advocates for the use of higher fidelity CFD approaches and additional measurements for a better understanding of flow regime effects. Notably, laminar flow dominance in calm water contrasts with increased turbulence observed in waves, emphasizing the significance of wave effects on propulsive factors and design. Overall, the results from this study provide insights into the physics of propeller flow in regular head waves, offering guidance to ship/propeller designers for optimizing designs in realistic environmental conditions beyond calm water. A very rough estimation of the total computational costs used for running the FT simulations in calm water and in regular head wave WC2 both with grid $n = 1.00$ at advance ratio $J \approx 0.55$ implies running on 256 cores (CPUs) for 60 hours and 100 hours, respectively.

3.5 Paper V

"Impacts of Regular Head Waves on Thrust Deduction at Model Self-Propulsion Point". Irannezhad, M., Kjellberg, M., Bensow, R. E., and Eslamdoost, A. (2024b). *Manuscript*

CRediT Authorship Contribution Statement

Mohsen Irannezhad: Conceptualization, Formal Analysis, Investigation, Data Curation, Writing – Original Draft, Writing – Review & Editing, Visualization. **Martin Kjellberg**: Conceptualization, Writing – Review & Editing, Supervision. **Rickard E. Bensow**: Conceptualization, Writing – Review & Editing, Supervision. **Arash Eslamdoost**: Conceptualization, Resources, Writing – Original Draft, Writing – Review & Editing, Supervision, Project Administration, Funding Acquisition.

Scope and Motivations

Paper V covers the last step towards the investigations of the propeller-hull interaction effects in calm water and regular head waves, shown in Section 1.4, through the analysis of a self-propelled hull performance using a RANS solver. In this paper, the performance of the self-propelled KVLCC2 in model-scale with a scale factor of 100 ($L = 3.2$ m) was studied. The investigated operational conditions in this paper were identical to the ones considered for the bare hull investigations in Paper III, while instead of a tow force F_0, the propeller rotational speed was adjusted (estimated) to obtain a near-to-zero mean surge motion during the spring response time, hence reaching a point very close to the self-propulsion point of the model (model SPP).

The main objective was to identify the impact of regular head waves on the propeller-hull interaction effects, in comparison to calm water condition.

Therefore, the bare hull and POW studies in Paper III and Paper IV were combined with the self-propulsion studies in this paper in order to investigate the propeller-hull interaction effects mainly through the thrust deduction and wake fraction analyses and also briefly through the analysis of the other propulsive factors, employing the thrust identity method. The impact of regular head waves on these propulsive factors was also briefly assessed through the comparison with the calm water condition.

The available experimental data from Osaka University Towing Tank, with the same spring system as of the bare hull model tests in Paper III, were used for validation of the computational results. In these experiments, the propeller slipstream velocity distribution measurements (SPIV) were performed on a plane fixed on the carriage 0.08 m ($0.025L$) behind the aft perpendicular. Since the primary objective of the experimental model tests was about the analysis of Energy Saving Devices (ESDs), an identical propeller rotational speed was considered in calm water and all three waves. Consequently, the propeller loading was different between CFD and EFD in different operational conditions, which substantially deteriorated the validation attempts. Given that the main objective in this paper concerned the numerical investigations at the self-propulsion point of the model, the simulations were divided into two main categories: one representing the model tests operational conditions in order to validate the results and another at the model SPP for the analysis of the propeller-hull interaction effects in line with the main objectives of this thesis.

Most of the simulation setups and post-processing techniques employed in this paper were similar to the ones explained in Paper III. Nevertheless, the self-propulsion simulations in Paper V consisted of a substantially larger number of cells and significantly smaller time steps.

In Paper V, the mean thrust deduction factor at the model SPP was calculated through modification of the thrust deficit/excess (from the estimated propeller rotational speed) by the mean spring and light-weight carriage forces ($-K\bar{x}^{SP} - m_3\bar{\ddot{x}}^{SP}$) as previously shown in Equation 2.31. This was because achieving the exact propeller rotational speed which yields zero mean surge was found to be practically impossible, due to the exceptionally large computational power requirements. However, since the spring and light-weight carriage forces were relatively insignificant, their effects on the main analyses carried out in Paper V were deemed inconsequential.

A discretized propeller was used in the simulations and the propeller rotation was mainly modeled using the Sliding Mesh technique, while a Moving Reference Frame (MRF) approach was used for the initialization of the simulations. Although larger time steps were considered during the application of the MRF approach, the time step was notably reduced for the final part of the simulations using the Sliding Mesh technique. Hence, the increased cell count as well as the adoption of smaller time steps in the Sliding Mesh technique in the self-propulsion simulations substantially increased the required computational costs in comparison to the bare hull investigations in Paper III.

Results and Conclusions

The thrust deduction factor, as one of the key investigated quantities, was derived involving a correction in its equation through the consideration of the thrust deficit/excess from the estimated propeller rotational speed to reach the model SPP at the intended velocity. The corrections were made through the relatively small retained spring system forces (related to the mean surge motion and acceleration) during a chosen time window of spring response time. Although this approach might not represent the full entailed physical effects at the model SPP, it is deemed to be a reasonably good approximation of it. While it is preferable to run the simulations for a longer physical time to obtain more accurate spring system behavior, the investigated status of the simulations in the current paper was found to be fairly adequate for the overall ship performance evaluation.

The CFD results were compared to the available experimental EFD data in selective operational conditions. Overall, the CFD results were comparable to the EFD data, particularly when the discrepancies were compared in terms of magnitude. The propeller slipstream transient velocity distribution was also compared qualitatively between CFD and 2-Dimensional Stereo Particle Image Velocimetry (SPIV) measurements.

The time series of different quantities from the CFD results in different waves were compared during one wave encounter period. Interestingly, the motions were almost identical between bare hull and self-propulsion conditions, hence the nominal wake analysis from the bare hull investigations in Paper III was used to analyze the propeller performance in self-propulsion condition in this paper. According to the bare hull studies, during one encountered wave period in regular head waves, substantial variations were seen for the axial velocity component of the surface-averaged nominal wake over the propeller disk $\tilde{u}$, and the time-averaged values $\bar{\tilde{u}}$ in all three waves were larger (around 9.8%, 21.3% and 14.6% for $\lambda/L = 0.6$, 1.1 and 1.6, respectively) than the calm water value. Overall, the variation of nominal wake in waves was found to be associated with the instantaneous propeller disk velocities, boundary layer contraction/expansion due to hull motions, bilge vortex dynamics, shaft vortex dynamics and the orbital wave velocities at the propeller disk as well as the complex interactions between these factors in different operational conditions. It was found that the large hull motions in the longer waves ($\lambda/L = 1.1$ and 1.6) dictated the variation of nominal wake through the contraction/expansion of the boundary layer as well as imposed vortical structure dynamics. However, the wave orbital velocities were the dominant factor in the shortest wave $\lambda/L = 0.6$ where the hull motions were insignificant.

The Taylor wake fraction was almost equal in all three wave lengths (and smaller than the calm water value), even though the propeller rotational speed was substantially different. Interestingly, the self-propulsion simulations and the applied thrust identity method yielded very similar values for the Taylor wake fraction in all three waves, in contrast to the nominal wake in bare hull condition. However, the Taylor wake fraction was decreased in all three waves compared to the calm water value, or in other words, the advance velocity

was increased in waves which was in line with the bare hull nominal wake observations.

The estimated thrust deduction factor in $\lambda/L = 0.6$, 1.1 and 1.6 was found to be respectively 12.8%, 26.1% and 12.9% smaller than the calm water value. The physical evidence of such reductions was discussed in this paper.

It was concluded that in $\lambda/L = 1.1$ and 1.6, due to very large shaft vertical motions and hence significant contraction/expansion of the boundary layer as well as strong vortical structure dynamics, the flow that was being ingested into the propeller during one encounter wave period was not solely and continuously from the aft ship boundary layer flow and hence, the wake had a larger momentum in comparison to the calm water wake which is heavily influenced by the hull boundary layer. Therefore, the incident flow to the propeller was expected to be substantially different and the primary acceleration of the flow and thus the impacts on the hull pressure distribution at the aft ship was not identical to the calm water condition. The diminished boundary layer flow acceleration and hence the less prominent change of pressure in the aft ship in self-propulsion in comparison to bare hull, in conjunction with the observed increase of $\bar{\bar{u}}$ in $\lambda/L = 1.1$ and 1.6 were the most likely physical evidence that led to the decrease of thrust deduction factor in these waves. More significant shaft vertical acceleration in $\lambda/L = 1.1$ and thus longer time period of bilge vortex residence outside of the propeller incident field resulted in a fuller wake (higher $\bar{\bar{u}}$ and thus less prone to be influenced by the propeller suction) in this wave in comparison to $\lambda/L = 1.6$, which was found to be the main reason for lower thrust deduction factor in $\lambda/L = 1.1$.

In $\lambda/L = 0.6$, due to the insignificant heave and pitch motions and hence smaller shaft vertical displacement, the aft ship pressure reduction, originated from the flow suction by the propeller, was rather concentrated on a roughly similar hull surface area as of calm water condition. On the one hand, the propeller rotational speed in this wave was larger than the calm water value to overcome the added resistance and reach the expected ship velocity at model SPP, which potentially can result in a more intense pressure reduction in the aft ship. On the other hand, a larger advance velocity was obtained in this wave versus calm water (due to the effects of the wave orbital velocities the nominal wake $\bar{\bar{u}}$ increased by 9.8% in comparison to calm water). These counteracting effects possibly have resulted in a reduction of the thrust deduction factor in this wave with respect to the calm water value.

It is worthwhile to mention that the analysis in this paper mainly concerned the global effects as the analysis of the local physical phenomena associated with the propeller performance in regular head waves was intricate because of the unsteady and complex effects of the flow at various radial and azimuthal positions on different blades during the encounter period in waves. However, in a brief single-blade thrust investigation during one encounter wave period, it was seen that the large shaft vertical motions in $\lambda/L = 1.1$ and 1.6 resulted in significant local effects that led to the swap of the minimum thrust generation of the blade between $\Theta \approx 90^\circ$ and $\Theta \approx 270^\circ$ azimuthal positions, based on the Cylindrical coordinate system presented in Figure 1 in Paper V.

Comments

The computational costs of running the simulations were extremely large, mainly due to the utilization of the discretized propeller and Sliding Mesh technique and hence a very small time step as well as the consideration of the ship free to surge utilizing a weak spring system. The latter increased the complexity of the problem and its post-processing techniques but with the advantage of obtaining more accurate ship performance results in regular head waves with an intended velocity compared to the fixed surge conditions. A rough approximation suggests that the calm water and the shortest wave self-propulsion simulations require 640 cores (CPUs) for 36 days (more than 550000 core-hours). However, for simulations in the longest wave, the cost increases by over 20%. This manuscript is under development and more analysis is in progress, which may lead to further revisions.

Chapter 4

Concluding Remarks

This thesis explored several steps to improve the general understanding of ship hydrodynamic performance in more realistic environmental conditions than the traditional calm water consideration. The objectives mainly focused on mapping the flow physics that contribute to propeller-hull interaction effects in regular head waves. This section aims to encapsulate the most significant findings of this study.

The bare hull investigations using the FNPF method were carried out in a broad range of operational conditions where an interesting behavior was observed for the added wave making resistance coefficient when it was plotted versus wave length. Despite the primary well-known peak of added wave making resistance coefficient near the wave lengths equal to the ship length, a secondary peak was detected in short waves when the wave length is close to the half ship length. From the FNPF investigation, the correlations between the ship motions and wave making resistance were studied to address such ship performance characteristics in various waves in a wider context.

The bare hull investigations by the RANS solver indicated a considerable (up to 6.8%) contribution of the added shear resistance to the total added resistance in wave, while the mean wetted surface area remained unchanged. This finding contradicted with the generally recognized assumption of equal frictional resistance in waves and calm water for estimating the skin friction correction force to unload the propeller at the self-propulsion point of the ship. The CFD investigations revealed significant variation of the surface-averaged nominal wake in regular head waves as well as severe fluctuations of the velocity distribution over the propeller disk. Moreover, the time-averaged of nominal wake in regular head waves indicated a significant dependency on the wave condition and demonstrated the potential to become substantially different than the calm water value, particularly in the wave condition where the added wave resistance was significant. The axial velocity component of the time-averaged nominal wake increased between 9.8% and 21.3% in different studied waves in comparison to calm water, whereas almost an identical Taylor wake fraction was seen in these waves from the self-propulsion condition. The Taylor wake fractions from the waves were about 12% lower than the calm water value

(fuller wake in waves) which implies a similar behavior as of the nominal wake. These were identified to be critically important for wake-adapted propeller design and optimization.

The propeller open water investigations by the RANS solver showed altered propeller performance in regular head waves in comparison to calm water which was mainly due to the change of flow regime on the blades, originating from the wave orbital velocities. All studied waves had a rather similar effect on the propeller open water characteristics, where for instance, the propeller open water efficiencies close to the best efficiency advance ratio were approximately 5% lower than the calm water value.

The propeller blade loading varies depending on the positioning of the blade within the wake in behind condition. Due to more vigorous wake dynamics in waves in comparison to calm water wake, the self-propulsion investigations by the RANS solver illustrated significant load variation on each blade during the wave encounter period, which might introduce design and material constraints for the propellers with respect to cavitation and noise.

The propeller-hull interactions are primarily conceived through the thrust deduction and wake fraction. It is a common practice to assume an equal thrust deduction factor and wake fraction for a ship operating in calm water and waves. Based on the systematic investigations carried out in this thesis for a ship in model-scale and operating at the self-propulsion point of the model in selective operational conditions in regular head waves, it was evidenced that this assumption does not hold in all conditions. A similar Taylor wake fraction was seen in different studied waves, which was around 12% lower than the calm water value. The thrust deduction factor was heavily dependent on the wave condition and for the waves under study in this thesis, it was reduced between 12.8% and 26.1% in comparison to the calm water value. The change of thrust deduction factor was found to be associated with the boundary layer contraction/expansion and vortical structure dynamics, originating from the wave orbital velocities as well as the significant shaft vertical motions and accelerations that resulted in a modified propeller action, and consequently diminished suction effect on the aft ship. The altered thrust deduction factor and wake fraction in waves in comparison to calm water underlines the significance of waves on the propulsive factors and propeller design.

Conducting investigations in free surge condition, by the means of a weak spring system, posed critical challenges not only to the simulation setup and its required computational costs, but also to the analysis and post-processing of the ship performance results. The effects on the computational costs of simulations were substantial, mainly due to the large required physical time of simulation for a better convergence and more accurate results post-processing. Nonetheless, the conducted free surge simulations in this thesis, denoting fewer simplifications and assumptions, provided a more accurate representation of the ship performance under more realistic conditions.

Overall, an overview of the ship motions and resistance in a wide range of operational conditions in regular head waves was achieved through the FNPF method, mainly due to its relatively lower computational costs. On the other hand, the employed CFD method was able to offer valuable insights into the

entailed flow physics in propeller-hull interaction effects in regular head waves and the deviations from calm water condition. Nevertheless, the computational costs associated with the CFD, particularly for the self-propulsion simulations, were exceedingly high. Therefore, the scope of investigations was heavily dependent on the available computing resources. It is recommended to initially use the FNPF method to identify the critical operational conditions in regular head waves and then employ higher fidelity CFD solvers to earn a deeper understanding of the flow physics in those operational conditions.

Last but not least, it should be mentioned that the majority of the propeller-hull interaction effects analyses and conclusions in this thesis concerned only the propeller-appended KVLCC2 in model-scale and solely under selective operational conditions, at the design speed, in fully-loaded loading condition, in calm water and three regular head waves, to name a few. Since the hull motions in head waves are primarily governed by pressure forces, most likely the full-scale motions would be rather similar to the motions obtained from the current model-scale study. However, the effects of boundary layer contraction/expansion and vortical structure dynamics would be reduced due to higher Reynolds numbers and hence the decline of viscous effects. Moreover, based on the observed dependency of the dynamics of the vortical structures and propeller slipstream on the characteristics of the encountered wave, the propeller-hull-rudder interactions may be subject to significant deviations in waves in comparison to calm water, which would result in rudder performance and vessel maneuverability deterioration and hence the overall ship performance degradation. Finally, performing similar investigations as of the current study, but in full-scale and/or other ships and operational conditions, and examining the effects of waves on the thrust deduction factor and wake fraction is highly recommended as a future work.

Bibliography

Berndt, J. C., Perić, R., and Abdel-Maksoud, M. (2021). "Improved Simulation of Flows with Free-Surface Waves by Optimizing the Angle Factor in the HRIC Interface-Sharpening Scheme". *Journal of Applied Fluid Mechanics* 14.3, pp. 909–920. ISSN: 1735-3572. https://doi.org/10.47176/jafm.14.03.32062.

Bertram, V. (2012). *Practical Ship Hydrodynamics*. Second. Oxford: Butterworth-Heinemann.

Bhattacharyya, A. and Steen, S. (2014). "Propulsive factors in waves: A comparative experimental study for an open and a ducted propeller". *Ocean Engineering* 91, pp. 263–272. ISSN: 0029-8018. https://doi.org/10.1016/j.oceaneng.2014.09.020.

Bhattacharyya, R. (1978). *Dynamics of Marine Vehicles*. A Wiley-Interscience publication. Wiley.

Cai, B., Mao, X., Xu, Q., Tian, B., Qiu, L., and Zhan, X. (2023). "Numerical simulation of KVLCC2 self-propulsion with ducted propeller in head waves". *Ocean Engineering* 285, p. 115427. ISSN: 0029-8018. https://doi.org/10.1016/j.oceaneng.2023.115427.

Eça, L. and Hoekstra, M. (2014). "A procedure for the estimation of the numerical uncertainty of CFD calculations based on grid refinement studies". *Journal of Computational Physics* 262, pp. 104–130. ISSN: 0021-9991. https://doi.org/10.1016/j.jcp.2014.01.006.

Eça, L., Vaz, G., Toxopeus, S. L., and Hoekstra, M. (2019). "Numerical Errors in Unsteady Flow Simulations". *Journal of Verification, Validation and Uncertainty Quantification* 4.2. 021001. ISSN: 2377-2158. https://doi.org/10.1115/1.4043975.

Eslamdoost, A., Irannezhad, M., and Bensow, R. E. (2023). "The Dynamics of a Ship Nominal Wake in Head Waves". In: *The 10th International Conference on Computational Methods in Marine Engineering (MARINE 2023)*. http://doi.org/10.23967/marine.2023.129.

Irannezhad, M. (2022). "Numerical investigation of ship responses in calm water and regular head waves". Thesis for the degree of Licentiate of Engineering, Report no. 2022:04, Department of Mechanics and Maritime Sciences, Chalmers University of Technology. ISSN: 1652-8565. https://research.chalmers.se/publication/530499/file/530499_Fulltext.pdf.

Irannezhad, M., Bensow, R. E., Kjellberg, M., and Eslamdoost, A. (2021). "Towards uncertainty analysis of CFD simulation of ship responses in regular

head waves". In: *Proceedings of the 23rd Numerical Towing Tank Symposium (NuTTS 2021)*. Duisburg, Germany, pp. 37–42. https://www.uni-due.de/imperia/md/content/ist/nutts_23_2021_mulheim.pdf.

Irannezhad, M., Bensow, R. E., Kjellberg, M., and Eslamdoost, A. (2023). "Comprehensive computational analysis of the impact of regular head waves on ship bare hull performance". *Ocean Engineering* 288. https://doi.org/10.1016/j.oceaneng.2023.116049.

Irannezhad, M., Eslamdoost, A., and Bensow, R. E. (2019a). "Numerical investigation of a general cargo vessel wake in waves". In: *Proceedings of the 22nd Numerical Towing Tank Symposium (NuTTS 2019)*. Tomar, Portugal. http://web.tecnico.ulisboa.pt/ist12278/NuTTS2019/Session1/Session1_2.pdf.

Irannezhad, M., Eslamdoost, A., and Bensow, R. E. (2019b). "Numerical investigation of a large diameter propeller emergence risk for a vessel in waves". In: *Proceedings of the 8th International Conference on Computational Methods in Marine Engineering (MARINE 2019)*. Gothenburg, Sweden, pp. 634–645. https://doi.org/10.5281/zenodo.2650219.

Irannezhad, M., Eslamdoost, A., Kjellberg, M., and Bensow, R. E. (2022a). "Investigation of ship responses in regular head waves through a Fully Nonlinear Potential Flow approach". *Ocean Engineering* 246. https://doi.org/10.1016/j.oceaneng.2021.110410.

Irannezhad, M., Kjellberg, M., Bensow, R. E., and Eslamdoost, A. (2022b). "Propeller open water characteristics in waves". In: *Proceedings of the 24th Numerical Towing Tank Symposium (NuTTS 2022)*. Zagreb, Croatia, pp. 36–41. https://drive.google.com/file/d/1Fw1qI6Fb9nQPP7p0QSAUMJ8yYRBBjYAy/view.

Irannezhad, M., Kjellberg, M., Bensow, R. E., and Eslamdoost, A. (2024a). "Experimental and numerical investigations of propeller open water characteristics in calm water and regular head waves". *Preprint Under Review in Ocean Engineering, available at SSRN*. http://doi.org/10.2139/ssrn.4706213. https://ssrn.com/abstract=4706213.

Irannezhad, M., Kjellberg, M., Bensow, R. E., and Eslamdoost, A. (2024b). "Impacts of Regular Head Waves on Thrust Deduction at Model Self-Propulsion Point". *Manuscript*.

ITTC (2014). International Towing Tank Conference. Recommended Procedures and Guidelines 7.5-03-03-01, "Practical Guidlines for Ship Self-Propulsion CFD", 27^{th} ITTC, 2014.

ITTC (2017a). International Towing Tank Conference. Recommended Procedures and Guidelines 7.5-02-03-01.5, "Predicting Powering Margins", 28^{th} ITTC, 2017.

ITTC (2017b). International Towing Tank Conference. Recommended Procedures and Guidelines 7.5-02-07-02.8, "Calculation of the weather factor f_w for decrease of ship speed in wind and waves", 28^{th} ITTC, 2017.

ITTC (2021a). International Towing Tank Conference. Final Report and Recommendations from the Seakeeping Committee, 29^{th} ITTC, 2021.

ITTC (2021b). International Towing Tank Conference. Final Report and Recommendations from the Specialist Committee on Modelling of Environmental Conditions, 29^{th} ITTC, 2021.

ITTC (2021c). International Towing Tank Conference. Recommended Procedures and Guidelines 7.5-02-02-01, "Resistance Test", 29^{th} ITTC, 2021.

ITTC (2021d). International Towing Tank Conference. Recommended Procedures and Guidelines 7.5-02-03-01.4, "1978 ITTC Performance Prediction Method", 29^{th} ITTC, 2021.

ITTC (2021e). International Towing Tank Conference. Recommended Procedures and Guidelines 7.5-02-07-02.1, "Seakeeping Experiments", 29^{th} ITTC, 2021.

ITTC (2021f). International Towing Tank Conference. Recommended Procedures and Guidelines 7.5-02-03-02.1, "Open Water Test", 29^{th} ITTC, 2021.

ITTC (2021g). International Towing Tank Conference. Dictionary of Hydromechanics, prepared by the Quality Systems Group of the 29^{th} ITTC, 2021.

ITTC (2021h). International Towing Tank Conference. Recommended Procedures and Guidelines 7.5-02-03-01.1, "Propulsion/Bollard Pull Test", 29^{th} ITTC, 2021.

ITTC (2021i). International Towing Tank Conference. Final Report and Recommendations from the The Resistance and Propulsion Committee, 29^{th} ITTC, 2021.

ITTC (2021j). International Towing Tank Conference. Recommended Procedures and Guidelines 7.5-02-07-02.2, "Prediction of Power Increase in Irregular Waves from Model Test", 29^{th} ITTC, 2021.

Kjellberg, M. (2013). "Fully non-linear unsteady three-dimensional boundary element method for ship motions in waves". PhD thesis. Chalmers University of Technology.

Korkmaz, K. B. (2023). "Assessment of Experimental, Computational, and Combined EFD/CFD Methods for Ship Performance Prediction". PhD thesis. Chalmers University of Technology.

Larsson, L. and Raven, H. C. (2010). *Ship Resistance and Flow.* PNA Series. Jersey City: Society of Naval Architects and Marine Engineers.

Lee, C.-M., Seo, J.-H., Yu, J.-W., Choi, J.-E., and Lee, I. (2019). "Comparative study of prediction methods of power increase and propulsive performances in regular head short waves of KVLCC2 using CFD". *International Journal of Naval Architecture and Ocean Engineering* 11.2, pp. 883–898. ISSN: 2092-6782. https://doi.org/10.1016/j.ijnaoe.2019.02.001.

Perić, R. and Abdel-Maksoud, M. (2018). "Analytical prediction of reflection coefficients for wave absorbing layers in flow simulations of regular free-surface waves". *Ocean Engineering* 147, pp. 132–147. ISSN: 0029-8018. https://doi.org/10.1016/j.oceaneng.2017.10.009.

Perić, R. and Abdel-Maksoud, M. (2020). "Reducing Undesired Wave Reflection at Domain Boundaries in 3D Finite Volume-Based Flow Simulations via Forcing Zones". *Journal of Ship Research* 64.01, pp. 23–47. ISSN: 0022-4502. https://doi.org/10.5957/jsr.2020.64.1.23.

Perić, R., Vukčević, V., Abdel-Maksoud, M., and Jasak, H. (2022). "Optimizing wave generation and wave damping in 3D-flow simulations with implicit relaxation zones". *Coastal Engineering* 171, p. 104035. ISSN: 0378-3839. https://doi.org/10.1016/j.coastaleng.2021.104035.

Roache, P. J. (1998). "Verification of Codes and Calculations". *AIAA Journal* 36.5, pp. 696–702. https://doi.org/10.2514/2.457.

Sadat-Hosseini, H., Wu, P.-C., Carrica, P., Kim, H., Toda, Y., and Stern, F. (2013). "CFD verification and validation of added resistance and motions of KVLCC2 with fixed and free surge in short and long head waves." *Ocean Engineering* 59, pp. 240–273. https://doi.org/10.1016/j.oceaneng.2012.12.016.

Saettone, S. (2020). "Ship Propulsion Hydrodynamics in Waves". PhD thesis. Technical University of Denmark. https://orbit.dtu.dk/en/publications/ship-propulsion-hydrodynamics-in-waves.

Seo, J.-H., Lee, C.-M., Yu, J.-W., Choi, J.-E., and Lee, I. (2020). "Power increase and propulsive characteristics in regular head waves of KVLCC2 using model tests". *Ocean Engineering* 216, p. 108058. ISSN: 0029-8018. https://doi.org/10.1016/j.oceaneng.2020.108058.

Sigmund, S. (2019). "Performance of ships in waves". PhD thesis. University of Duisburg-Essen. https://doi.org/10.17185/duepublico/70021.

Ueno, M., Tsukada, Y., and Tanizawa, K. (2013). "Estimation and prediction of effective inflow velocity to propeller in waves". *Journal of Marine Science and Technology* 18, pp. 339–348. https://doi.org/10.1007/s00773-013-0211-8.